NACA

RESEARCH MEMORANDUM

SUMMARY OF FREE-FLIGHT ZERO-LIFT DRAG RESULTS FROM TESTS OF 1/5-SCALE MODELS OF THE CONVAIR YF-102 AND F-102A AIRPLANES AND SEVERAL RELATED SMALL EQUIVALENT BODIES AT MACH NUMBERS FROM 0.70 TO 1.46

By Harvey A. Wallskog

Langley Aeronautical Laboratory
Langley Field, Va.

NATIONAL ADVISORY COMMITTEE
FOR AERONAUTICS

WASHINGTON

OCT 29 1954

NATIONAL ADVISORY COMMITTEE FOR AERONAUTICS

RESEARCH MEMORANDUM

for the

U. S. Air Force

SUMMARY OF FREE-FLIGHT ZERO-LIFT DRAG RESULTS FROM TESTS OF 1/5-SCALE MODELS OF THE CONVAIR YF-102 AND F-102A AIRPLANES AND SEVERAL RELATED SMALL EQUIVALENT BODIES AT MACH NUMBERS FROM 0.70 TO 1.46

By Harvey A. Wallskog

SUMMARY

One-fifth-scale rocket-propelled models of the Convair YF-102 and F-102A airplanes were tested to determine free-flight zero-lift drag coefficients through the transonic speed range at Reynolds numbers near those to be encountered by the full-scale airplane. Trim and duct characteristics were obtained along with measurements of total-, internal-, and base-drag coefficients. Additional zero-lift drag tests involved a series of small equivalent-body-of-revolution models which were launched to low supersonic speeds by means of a helium gun. The several small models tested corresponded to the following full-scale airplanes: basic, YF-102, 2-foot (full-scale) fuselage extension, F-102A, F-102A (relocated inlets), F-102A (faired nose), and F-102A (parabolic nose). Equivalent-body models corresponding to the normal area distribution (derived for Mach number 1.0) of each of these airplane shapes were flown and, in addition, equivalent-body models designed to represent the YF-102 and F-102A airplanes at Mach number 1.2 were tested.

External-drag coefficients obtained from the 1/5-scale tests ranged from 0.0094 to 0.0273 for the YF-102 model and from 0.0100 to 0.0255 for the F-102A model. Forebody external-pressure-drag coefficients (drag rise) at Mach number 1.05 of 0.0183 and 0.0154 were obtained from the 1/5-scale models of the YF-102 and F-102A, respectively, a 16-percent reduction for the F-102A model. Values of drag rise at Mach number 1.05 from the small equivalent-body tests were nearly the same for the basic, YF-102, and 2-foot-fuselage-extension airplane shapes. Equivalent-body

tests of the YF-102 and F-102A shapes showed the latter to have about 25 percent less drag rise as compared with a 16-percent reduction illustrated by the 1/5-scale tests. Additional equivalent-body tests illustrating effects of modifications to the F-102A airplane shape showed that relocating the inlets on the fuselage or altering the nose shape to provide a smoother cross-sectional area progression reduced the drag rise by approximately 16 percent. Replacing a major portion of the nose of the F-102A equivalent-body model with one of parabolic shape resulted in about a 21-percent reduction in drag rise. The drag-rise data from the equivalent-body tests include base drag.

INTRODUCTION

The Convair F-102 configuration has been the subject of many tests made in the Naval Ordnance Laboratory 40- by 40-cm Aeroballistics Tunnel (ref. 1) and the Southern California Cooperative Wind Tunnel (ref. 2) by Convair and in the Langley 4- by 4-foot supersonic pressure tunnel (ref. 3) and the Langley 8-foot transonic tunnel (refs. 4 and 5) by the National Advisory Committee for Aeronautics. These tests, using small-scale models (1/20 scale and smaller), were performed to determine static stability, drag due to lift, and zero-lift drag of the basic (interim) airplane.

Presented herein are data obtained from two 1/5-scale models of the Convair F-102 configuration which were tested in free flight by the rocket-model technique. These 1/5-scale models were designed and instrumented to obtain free-flight, near-zero-lift measurements of total-, internal-, and base-drag coefficients through the transonic speed range at Reynolds numbers comparable to those encountered by the full-scale airplane. One model corresponded closely to the prototype airplane (final sharp nose and canopy). The data from this model were reported in reference 6 as the 1/5-scale rocket-propelled model configuration and are repeated in this paper under the designation YF-102. The second 1/5-scale model test corresponded to the F-102A airplane. Both models tested had wings with NACA 0004-65 (modified) airfoil sections and no twist or camber. Because of the large number of modified configurations tested, no comparisons with wind-tunnel data were attempted.

In addition to the 1/5-scale tests, nine small equivalent bodies of revolution were tested in free flight by using the helium gun. These small equivalent-body models were flown as a quick and simple means to determine the relative magnitude of the transonic drag rise of the various modified versions of the F-102 configuration. The data from models 1 to 6 were presented in reference 6.

All models were designed (with the collaboration of the NACA) and built by Convair. All tests were conducted by the Langley Pilotless

Aircraft Research Division and flight testing took place at the Langley Pilotless Aircraft Research Station at Wallops Island, Va. The present tests are a continuation of a research project conducted at the request of the U. S. Air Force.

SYMBOLS

X	longitudinal distance along body axis from station 0, in.
L	distance from station 0 to exit, in.
A	cross-sectional area of the particular configuration as determined by the intersecting Mach plane, sq in.
S	wing plan-form area obtained by extending leading and trailing edges to center line of body, $S = 26.46$ sq ft for 1/5-scale models and equivalent, $S = 0.1786$ sq ft for equivalent-body models
S_b	base area of central body in duct, sq ft
A_i	inlet area (interior, total for 2 inlets), sq ft
A_e	exit area, sq ft
$\bar{c}$	mean aerodynamic chord, ft
α	angle of attack, deg
β	angle of sideslip, deg
M	Mach number
q	free-stream dynamic pressure, lb/sq ft
R	Reynolds number, based on $\bar{c}$ for 1/5-scale models and $L/12$ for equivalent-body models
C_D	total drag coefficient, $\frac{\text{Total drag force}}{qS}$
C_{N_t}	trim normal-force coefficient, $\frac{\text{Trim normal force}}{qS}$

C_{Y_t} trim side-force coefficient, $\frac{\text{Trim side force}}{qS}$

H_i total pressure at center of inlet, lb/sq ft

H_e average total pressure across duct near exit, lb/sq ft

H_o free-stream total pressure, lb/sq ft

H_i/H_o inlet total-pressure recovery

H_e/H_o total-pressure recovery at duct exit

p free-stream static pressure, lb/sq ft

p_b base pressure (on base of duct central body only), lb/sq ft

C_{p_b} base pressure coefficient, $\frac{p_b - p}{q}$

C_{D_b} base-drag coefficient, $-C_{p_b}S_b/S$

M_e Mach number at duct exit

p_e static pressure at duct exit, lb/sq ft

γ ratio of specific heats for air

m/m_o mass-flow ratio ($\gamma = 1.40$), $\frac{p_e M_e A_e}{pMA_i}\left(\frac{1 + 0.2M_e^2}{1 + 0.2M^2}\right)^{1/2}$

C_{D_I} internal-drag coefficient ($\gamma = 1.40$),

$$2\frac{m}{m_o}\frac{A_i}{S}\left[1 - \frac{M_e}{M}\left(\frac{1 + 0.2M^2}{1 + 0.2M_e^2}\right)^{1/2}\right] - \frac{(p_e - p)}{q}\frac{A_e}{S}$$

C_{D_f} friction-drag coefficient

C_{D_E} forebody external-drag coefficient, $C_D - C_{D_I} - C_{D_b}$

C_{D_p} forebody external-pressure-drag coefficient, $C_D - C_{D_I} - C_{D_b} - C_{D_f}$

$C_{D_{p+b}}$ external-pressure-drag coefficient, $C_D - C_{D_I} - C_{D_f}$ for 1/5-scale models and $C_D - C_{D_f}$ for equivalent-body models

MODELS AND TESTS

1/5-Scale Models

Drawings showing the general arrangement of the two 1/5-scale rocket-propelled models appear in figure 1, pertinent physical characteristics are listed in table I, and airfoil ordinates are given in table II. Weight, balance, and inertia data are presented in table III. The longitudinal distribution of cross-sectional area derived for Mach number 1.0 (Mach planes normal to the reference line) for each model is shown in figure 2. Photographs of the YF-102 and F-102A models are shown as figure 3.

The model of the YF-102 airplane corresponded closely to the prototype airplane (final nose shape and sharp canopy) with the exception that the rear portion of the fuselage was slightly enlarged and lengthened in order to simulate provision for a different engine. The model of the F-102A airplane was designed to correspond as closely as possible to the production airplane with the exception that the model tested had a wing without twist or camber. The only difference between the two 1/5-scale models tested was in the shape of the fuselage rearward of the canopy. In order to obtain improved performance at transonic and low supersonic speeds, the fuselage of the F-102A airplane was lengthened and reshaped to provide a more favorable distribution of cross-sectional area over the previous design.

For both models the wings had 60° sweptback leading edges, 5° swept-forward trailing edges, and used NACA 0004-65 (modified) streamwise airfoil sections. The vertical tail of each model was similar in plan form and section to a wing semispan. To obtain near-zero lift longitudinal trim the elevons of the YF-102 model were preset with a deflection of approximately 1.3° trailing edge up and those of the F-102A model were set 1.5°. Both models had 0° rudder deflection.

Each of the 1/5-scale rocket-propelled models had an internal duct in the form of a Y where the branches merged a short distance behind the inlets to form a large single duct which surrounded the internal rocket motor. The twin side inlets of each model were scaled from the airplane inlets designed for the Wright J-67 engine. In order to provide a choked exit in each model, a conical-shaped sleeve was attached to the internal-rocket-motor nozzle at the exit, thus providing an annular exit (see

figs. 3(c) and 4). The sleeves were designed to provide a ratio of exit area to inlet area of 1.0, where the reference inlet was taken as the cross-sectional area in a plane normal to the duct axis at the most forward station where the interior contour is fully developed. The canopy, inlets, control-actuator housings, and drogue-parachute housing (and wing fences for the YF-102 model) were all scaled from the respective airplanes. Each model was covered with a heat-resistant, phenolic-resin-base paint.

Two-stage propulsion systems, utilizing solid-fuel rocket motors, were used to launch each model from the ground and accelerate it to supersonic speeds. A photograph of the F-102A model and booster-rocket combination taken just before launching appears in figure 3(d). A single high-performance air-to-ground (HPAG) rocket was used for the booster of the YF-102 model, whereas two HPAG rockets were used for the F-102A model in order to compensate for its greater weight and provide a slightly higher maximum Mach number. The booster propelled each model to a low subsonic speed at which time it separated from the model and the internal rocket motor (6-inch ABL Deacon rocket motor) was ignited and accelerated the model up to maximum speed. The data contained herein were recorded during the period after the internal-rocket-motor propellant of each model was expended when the models were in free flight.

Equivalent-Body Models

Presented in figure 5 is a drawing of a typical equivalent-body-of-revolution model showing the size and shape of the stabilizing fins. Equivalent-body models 1 to 9 correspond to the following full-scale airplanes or modified versions thereof:

	Model
Basic (Convair designation)	1
YF-102	2
2-foot fuselage extension (from basic)	3
F-102A (referred to as 7-foot fuselage extension in ref. 6)	4
YF-102 (M = 1.2 area distribution)	5
F-102A (M = 1.2 area distribution; this model referred to as 7-foot fuselage extension in ref. 6)	6
F-102A (relocated inlets)	7
F-102A (faired nose)	8
F-102A (parabolic nose)	9

Except where noted, the equivalent-body models were designed by the transonic (M = 1.0) area-rule concept (ref. 7), that is, the cross-sectional areas (fig. 6) were determined by planes intersecting the

airplane perpendicular to the reference axis. Models 5 and 6 were designed to investigate the possibility of determining the wave drag of the YF-102 and F-102A airplanes at $M = 1.2$ by means of a single equivalent body of revolution for each. As stated by Jones in reference 8 and Whitcomb and Fischetti in reference 9, a concept has been developed for inter-relating the wave drag of wing-body combinations at moderate supersonic speeds with axial distributions of cross-sectional area. By this concept the wave drag of an airplane configuration is related to a number of distributions of the normal components of cross-sectional areas as intersected by Mach planes which are inclined to the stream at the Mach angle. The various distributions are obtained with the axis of tilt of these Mach planes rolled to various positions around the center line of the configuration. For the present tests this concept was further simplified by the assumption that the wave drag of the configuration would be approximated by the wave drag of a single body of revolution which was shaped to correspond to the average of the 10 distributions obtained by placing the Mach planes at 10 angles of roll from 0° to 180° around the configuration reference line.

In order to simulate each airplane at the condition of mass-flow ratio of 1.0, the duct inlet area was subtracted from each model total area distribution at stations along the body axis from the inlet to the exit. From these net area distributions the cross-sectional area distribution of the equivalent-body-model stabilizing fins was removed.

The models were machined in two parts, a steel nose and an aluminum afterbody. The hexagonal-section, swept stabilizing fins were made of duralumin and pinned in place. Photographs of typical equivalent-body models appear as figure 7.

The models were launched to supersonic speeds by using the helium gun which is described in reference 10.

INSTRUMENTATION AND DATA REDUCTION

1/5-Scale Models

The 1/5-scale rocket-propelled model of the YF-102 airplane was equipped with an eight-channel telemeter contained within the body which transmitted continuous measurements of longitudinal, normal and transverse accelerations, free-stream, duct-inlet, and duct-exit total pressures, and static pressures in the duct at the exit and on the base of the duct central body. The three accelerometers were located near the model center of gravity, and the total-pressure probe in the duct near the exit was a slotted, integrating rake spanning the duct (see

fig. 4). The 1/5-scale model of the F-102A was instrumented in like manner except that longitudinal-acceleration and free-stream total-pressure channels using low-range instruments were added in order to improve the accuracy of the data at subsonic speeds. Other instrumentation used to record necessary information consisted of an NACA modified SCR584 radar tracking unit used to obtain trajectories and radiosonde units used to measure air pressure and temperature from which the local values of the speed of sound, density, and viscosity at altitude were obtained.

Model airspeeds, Mach numbers, Reynolds numbers, and dynamic pressures were calculated from telemetered values of free-stream total pressures and ambient pressures and temperatures from the radiosonde survey. Longitudinal-, normal-, and side-force coefficients (C_D, C_{N_t}, and C_{Y_t}, respectively) were obtained by using telemetered values of acceleration. Deviations from the standard methods of data reduction are explained in the following paragraphs.

In the case of the data from the YF-102 model, the measurements of duct-inlet total pressure and duct-exit static pressure were of questionable quality and hence were not used. Total-pressure-recovery data at the duct exit (H_e/H_o) are presented because of the lack of inlet total-pressure data. In order to calculate values of mass-flow ratio and internal-drag coefficient, the following assumptions were made concerning the duct-exit static pressure p_e and duct-exit Mach number M_e (for $\gamma = 1.40$):

For $M > 1.0$,

$$p_e = 0.5283H_e$$

$$M_e = 1.0$$

and for $M < 1.0$,

$$p_e = p_b$$

$$\frac{p_e}{H_e} = \left(1 + 0.2M_e^2\right)^{-7/2}$$

For the YF-102 model the telemetered signal corresponding to the longitudinal-acceleration instrument apparently suffered an abrupt shift and a drift in frequency which was proportional to acceleration. The magnitude of the shift and drift in acceleration was calculated by using the subsonic drag level obtained from the free-flight test of the large-scale model of the F-102A. By using these data (after adjustment for a

difference in external surface area) at two subsonic Mach numbers and by applying the actual test conditions of the YF-102 model, it was possible to correct the telemetered values of longitudinal acceleration. By comparing the calculated and telemetered values of longitudinal acceleration at the two subsonic Mach numbers and assuming the drift rate to be constant, it was possible to calculate the shift and drift rate which occurred in flight.

When the data from the YF-102 model were presented in reference 6 (under the designation 1/5-scale rocket-propelled model), the data from the F-102A model were not available. Hence, in order to perform the necessary adjustment of the data, the only available data for this airplane shape were used (unpublished data from the Langley 8-foot transonic tunnel). Since the wind-tunnel model data appeared to be low (after adjustment for different Reynolds numbers) by comparison to the later rocket-propelled model data, it seemed advisable to change the basis for adjustment of the YF-102 model drag data to the F-102A rocket-propelled model (present results). It is felt that the effect of a different surface finish may be the primary reason for disagreement between the 1/5-scale, free-flight test results and the wind-tunnel data.

In the case of the 1/5-scale model of the F-102A airplane, the only difficulty encountered was with the telemetered values of the duct-exit total pressure at speeds below $M = 0.9$. In view of this, the curves of total-pressure recovery at the duct exit H_e/H_o, mass-flow ratio m/m_o, and internal-drag coefficient C_{D_I} were extrapolated from $M = 0.9$ to the low-speed end. The extrapolated curve of internal-drag coefficient, being the most easily established, was used as a guide to determine the curves of m/m_o and H_e/H_o.

The total-drag-coefficient data presented herein are believed to be accurate to within the following limits:

Model	C_D	M
1/5-scale YF-102	± 0.0012	± 0.010
1/5-scale F-102A	$\pm .0007$	$\pm .010$

In general, errors in total-drag-coefficient curves stem from nonrandom sources which could cause the total-drag data from any one particular test to be consistently high or consistently low. These errors are minimized when pressure-drag data are obtained and, therefore, it is believed that the forebody external-pressure-drag-coefficient data presented herein are more accurate than the total-drag data. For this

reason, it is believed that adjustment of the telemetered longitudinal-acceleration data from the YF-102 model in the manner described previously had little detrimental effect on the measurement of the drag rise (forebody external-pressure-drag coefficients).

Equivalent-Body Models

Data were obtained from the small equivalent-body models by the use of a CW Doppler radar unit which was located on the ground next to the helium gun. Total drag coefficients and Mach numbers were determined by means of radar data and measured ground pressure and temperature by the method described in reference 11.

The total-drag data from the equivalent-body models are estimated from experience with previous models to be accurate within 0.0010 in C_D and 0.010 in M.

RESULTS AND DISCUSSION

Flight Reynolds numbers based on wing mean aerodynamic chord $\bar{c}$ for the 1/5-scale models and longitudinal distance L/12 for each of the nine equivalent-body models are presented in figure 8.

Friction-drag coefficients over the Mach number range were estimated from the measured Reynolds number variation and compressible skin-friction coefficients obtained from reference 12 and the resulting curves were adjusted to the individual subsonic drag level for all models in order to determine the magnitude of pressure-drag coefficients at supersonic speeds.

1/5-Scale Models

The basic data obtained from the flight tests of the 1/5-scale rocket-propelled models are presented in figures 9 to 11 for the YF-102 model and in figures 12 to 14 for the F-102A model.

Illustrated in figures 9 and 12 are the measured drag characteristics of the YF-102 and F-102A models, respectively. Curves of total-, internal-, base-, and external-drag coefficients are shown for the Mach number range along with estimated friction-drag coefficients. The total-drag-coefficient curve for the YF-102 model, presented in figure 9(a), was established in part by using the subsonic external-drag data from the 1/5-scale test of the F-102A (see section entitled, "INSTRUMENTATION AND DATA REDUCTION"). Nearly constant values of internal-drag coefficient were obtained over the entire Mach number range of the tests. Relatively low values of internal

drag (0.0005 to 0.0007) were expected because of the large increase in duct area behind the inlets and because of the smooth variations in duct area. Base-drag coefficients ranged from -0.0007 at high subsonic speeds to a maximum of 0.0020 at $M \approx 1.3$ for the YF-102 model and from -0.0007 at high subsonic speeds to 0.0005 at $M \approx 1.45$ for the F-102A model. Base pressures for each model, however, were measured only on the portion of the base which was formed by the central body in the duct, that is, the base of the sleeve and the exit of the internal rocket motor (fig. 3(c)). Since base pressures were not measured on the annular area of the base of the fuselage at the duct-exit station for either model, the forebody external-drag data of figures 9(b) and 12(b) include a small amount of drag due to this base area. Base-pressure coefficients are shown in figures 10 and 13 for the YF-102 and F-102A models, respectively.

Illustrated in figures 11 and 14 are the trim normal- and side-force coefficients and duct characteristics obtained from the flight tests of the 1/5-scale models. The elevons of the YF-102 model were preset with a deflection of approximately 1.3° trailing edge up and those of the F-102A model were set 1.5°. Both models had 0° rudder deflection.

Each model exhibited an abrupt change in C_{N_t} in the vicinity of $M = 0.95$. These low-lift longitudinal-trim changes correspond to changes in trim angle of attack of $1/2^\circ$ or less and probably would be hardly noticeable to the pilot because of changing stability and control effectiveness in the lift-coefficient range at which the airplane flies. These trim changes undoubtedly result from strong shock waves present near the wing trailing edge and fuselage afterbody at transonic speeds as illustrated by the schlieren photographs in reference 4.

The C_{Y_t} curve from the YF-102 model was smooth through the Mach number range, whereas that from the F-102A model showed an abrupt break near $M = 0.96$. The reason for the sharp break in the lateral-trim curve at transonic speeds for the F-102A model is not apparent at this time. A maximum change in trim angle of sideslip at transonic speeds for the 1/5-scale model of the F-102A was estimated to be nearly 1° and, if attributable to the configuration, illustrates what may be an undesirable airplane flight characteristic.

The inlets of each model were shaped the same and each had a choked exit. The mass-flow ratios m/m_o exceed 1.0 in both cases primarily because the interior inlet areas were used in the calculations (see table I).

Presented in figure 15 are the forebody external-pressure-drag coefficients C_{D_p} obtained from the YF-102 and F-102A models. The

values of C_{D_p} from the YF-102 model decrease slightly with Mach number after reaching a maximum at $M = 1.0$, whereas those from the F-102A model reach a maximum at $M \approx 1.25$. The values of C_{D_p} (drag rise) at $M = 1.05$ were 0.0183 and 0.0154 for the YF-102 and F-102A models, respectively.

Equivalent-Body Models

The total-drag-coefficient curves presented in figure 16 were obtained from free-flight tests of nine equivalent-body-of-revolution models which represented several variations of the Convair F-102 configuration. The shapes of models 1 to 4 and 7 to 9 were determined from the transonic ($M = 1.0$) distribution of cross-sectional area of the respective airplanes. In an attempt to evaluate the drag of two of the airplane shapes at $M = 1.2$, the contractor supplied two equivalent bodies which were shaped to correspond to area distributions of the airplanes derived for $M = 1.2$ as discussed in the section entitled "MODELS AND TESTS." The results of these tests (models 5 and 6) are also shown in figure 16. Presented also in figure 16 are the estimated friction-drag coefficients used to determine drag-rise increments. In order to illustrate the drag penalty associated with flight through transonic speeds and to minimize the effects of Mach number error, drag-rise values listed in table IV are for $M = 1.05$ for the transonic-area-distribution models. Drag-rise values for models 5 and 6 were obtained at $M = 1.2$. All drag-rise values include base drag. Corresponding values of drag rise (including base drag at the specified Mach number) from the 1/5-scale tests are included in table IV.

For models 1, 2, and 3, the relatively small differences in fuselage shape produced no significant changes in drag rise at transonic speeds. The data from model 4, however, indicated about a 25-percent reduction in drag rise from that shown by model 2. Drag-rise values obtained from the equivalent-body tests of the YF-102 and F-102A airplanes (models 2 and 4) were approximately 96 and 92 percent, respectively, of the values indicated by the 1/5-scale tests. The $M = 1.2$ equivalent bodies of the YF-102 and F-102A airplanes (models 5 and 6), however, had values of drag rise at $M = 1.2$ of only approximately 81 and 70 percent, respectively, of the magnitudes shown by the 1/5-scale tests. It appears that, from the results of models 5 and 6, attempting to represent a complete airplane in the form of a single equivalent body of revolution is not feasible for Mach numbers greater than 1.0, that is, where this single body-of-revolution shape is obtained from the average of the areas at each station of the many bodies determined by rotation of the inclined Mach planes around the longitudinal axis. Models 7 and 8 were designed to illustrate what reduction in drag of the F-102A airplane would occur if the area distribution in the vicinity of the inlets and canopy were smoothed out. The drag-rise values listed in table IV for the equivalent-body models

show that relocating the inlets (model 7) and fairing the nose to eliminate the depression in the area distribution (model 8) (see fig. 6(d)) both provided a substantial (16-percent) reduction in drag rise. Model 9 was designed to show the effect of replacing the major portion of the nose of the F-102A equivalent body with a parabolic shape. This change provided about a 21-percent reduction in equivalent-body drag rise at transonic speeds.

CONCLUSIONS

One-fifth-scale models of two versions of the Convair F-102 configuration were tested in free flight in order to evaluate zero-lift drag coefficients through the transonic speed range at high Reynolds numbers. Nine small equivalent-body-of-revolution models representing several variations of the airplane were also flight-tested to determine zero-lift drag rise.

1. External-drag coefficients (total minus internal minus base drag) obtained from the 1/5-scale YF-102 model were 0.0094 (minimum) at subsonic speeds and 0.0273 (maximum) at a Mach number of 1.0. From the 1/5-scale model test of the F-102A airplane the external-drag coefficients were 0.0100 (minimum) at subsonic speeds and 0.0255 (maximum) at a Mach number of 1.2.

2. Forebody external-pressure-drag coefficients (drag rise) at a Mach number of 1.05 were 0.0183 and 0.0154 from the 1/5-scale tests of the YF-102 and F-102A models, respectively, indicating the F-102A model (modified area distribution) has 16 percent less drag rise at a Mach number of 1.05 than the YF-102.

3. Drag-rise values obtained from the small equivalent-body tests of the YF-102 and F-102A airplanes were approximately 96 and 92 percent, respectively, of the values obtained from the 1/5-scale tests. These comparisons were made by using data which included base drag.

4. Data from the equivalent-body model of F-102A indicated a 25-percent reduction in drag rise from that obtained from the YF-102 equivalent-body model as compared with 16 percent obtained from the 1/5-scale tests.

5. For the small equivalent-body models designed to correspond to the airplane area distributions at a Mach number of 1.0, the relatively small differences in fuselage shape of the basic, YF-102, and 2-foot-fuselage-extension models produced no significant changes in drag rise at transonic speeds.

6. Additional equivalent-body tests of the F-102A airplane shape showed that relocating the inlets on the fuselage or altering the fuselage shape to provide a faired nose (i.e., smooth area progression) reduced the drag rise of the equivalent body by approximately 16 percent. Replacing a major portion of the nose of the F-102A equivalent-body model with one of parabolic shape resulted in about a 21-percent reduction in drag rise.

Langley Aeronautical Laboratory,
National Advisory Committee for Aeronautics,
Langley Field, Va., October 13, 1954.

Harvey A. Wallskog.

Harvey A. Wallskog
Aeronautical Research Scientist

Approved:

Joseph A. Shortal

Joseph A. Shortal
Chief of Pilotless Aircraft Research Division

JKS

REFERENCES

1. O'Brien, N. R., and Oakes, W. J.: Supersonic Wind Tunnel Tests of an .016 Scale Model of the F-102 Airplane in the NOL 40cm x 40cm Wind Tunnel. Part I: Evaluation of the Preliminary Configuration. Aero Memo A-8-17 (Contract No. AF 33(600)-5942), Consolidated Vultee Aircraft Corp., May 16, 1952.

2. O'Brien, Norman R.: Summary of Wind Tunnel Test Results for the F-102 Airplane at Mach 1.20 in the Coop Wind Tunnel Utilizing a 1/20th Scale Model. Aero Memo A-8-8 (Revision A), Consolidated Vultee Aircraft Corp., Feb. 20, 1952.

3. Hilton, John H., Jr., Hamilton, Clyde V., and Lankford, John L.: Preliminary Wind-Tunnel Investigation of a $\frac{1}{20}$-Scale Model of the Convair MX-1554 at Mach Numbers of 1.61 and 2.01. NACA RM SL52L11a, U. S. Air Force, 1952.

4. Osborne, Robert S., and Wornom, Dewey E.: Aerodynamic Characteristics Including Effects of Wing Fixes of a 1/20-Scale Model of the Convair F-102 Airplane at Transonic Speeds. NACA RM SL54C23, U. S. Air Force, 1954.

5. Osborne, Robert S., and Tempelmeyer, Kenneth E.: Longitudinal Control Characteristics of a 1/20-Scale Model of the Convair F-102 Airplane at Transonic Speeds. NACA RM SL54G15, U. S. Air Force, 1954.

6. Wallskog, Harvey A.: Free-Flight Zero-Lift Drag Results From a 1/5-Scale Model and Several Small-Scale Equivalent Bodies of Revolution of the Convair F-102 Configuration at Mach Numbers up to 1.34. NACA RM SL54D09b, U. S. Air Force, 1954.

7. Whitcomb, Richard T.: A Study of the Zero-Lift Drag-Rise Characteristics of Wing-Body Combinations Near the Speed of Sound. NACA RM L52H08, 1952.

8. Jones, Robert T.: Theory of Wing-Body Drag at Supersonic Speeds. NACA RM A53H18a, 1953.

9. Whitcomb, Richard T., and Fischetti, Thomas L.: Development of a Supersonic Area Rule and an Application to the Design of a Wing-Body Combination Having High Lift-to-Drag Ratios. NACA RM L53H31a, 1953.

10. Hall, James Rudyard: Comparison of Free-Flight Measurements of the Zero-Lift Drag Rise of Six Airplane Configurations and Their Equivalent Bodies of Revolution at Transonic Speeds. NACA RM L53J21a, 1954.

11. Stoney, William E., Jr.: Some Experimental Effects of Afterbody Shape on the Zero-Lift Drag of Bodies for Mach Numbers Between 0.8 to 1.3. NACA RM L53I01, 1953.

12. Van Driest, E. R.: Turbulent Boundary Layer in Compressible Fluids. Jour. Aero. Sci., vol. 18, no. 3, Mar. 1951, pp. 145-160, 216.

TABLE I

DIMENSIONAL DATA FOR THE 1/5-SCALE ROCKET-PROPELLED MODELS OF THE CONVAIR YF-102 AND F-102A AIRPLANES

Wing: (Same for both models)		
Area, total, sq ft	26.46	
Span, in.	91.5	
Mean aerodynamic chord, in.	55.5	
Aspect ratio, total	2.2	
Taper ratio	0	
Root chord, in.	83.3	
Tip chord, in.	0	
Airfoil section	NACA 0004-65 (modified)	
Angle of incidence, deg	0	
Dihedral angle, deg	0	
Sweepback, leading edge, deg	60	
Sweepforward, trailing edge, deg	5	
Elevon area, total, sq ft	2.63	
Elevon deflection, average, trailing edge up, deg		
YF-102	1.3	
F-102A	1.5	
Vertical tail: (Same for both models)		
Area, exposed, sq ft	2.73	
Span, panel, in.	20.8	
Aspect ratio, panel	1.1	
Taper ratio	0	
Root chord, in.	37.8	
Tip chord, in.	0	
Airfoil section	NACA 0004-65 (modified)	
Sweepback, leading edge, deg	60	
Sweepforward, trailing edge, deg	5	
Fuselage:	YF-102	F-102A
Length, overall, in.	123.4	137.9
Width, maximum, in.	15.6	15.6
Height, maximum:		
With canopy, in.	16.5	16.5
Without canopy, in.	15.6	15.6
Base area:		
Total, sq in.	90.1	53.5
Central body in duct exit, sq in.	53.2	24.6
Duct:		
Inlet area (interior, $\alpha \approx 5^{\circ}$, $\beta = 0^{\circ}$), measured, sq in.	26.8	27.4
Inlet area (inlet lip contour projected on plane normal to reference line), design, sq in.	29.3	29.3
Exit area ($\alpha \approx 2^{\circ}$, $\beta = 0^{\circ}$), sq in.	26.8	27.4

TABLE II

ORDINATES OF THE NACA 0004-65 (MODIFIED) AIRFOIL SECTION

FOR THE 1/5-SCALE ROCKET-PROPELLED MODELS

Station, percent chord	Ordinate, percent chord
0	0
.25	.281
.50	.389
.75	.468
1.00	.532
1.25	.587
2.50	.788
5.00	1.034
7.50	1.196
10.00	1.319
15.00	1.501
20.00	1.636
25.00	1.744
30.00	1.832
35.00	1.902
40.00	1.955
45.00	1.988
50.00	2.000
55.00	1.997
60.00	1.977
65.00	1.924
70.00	1.821
75.00	1.652
80.00	1.400
85.00	1.064
90.00 ↓ 100.00	(a)
L.E. radius, 0.176 percent chord T.E. radius, 0.013 inch	

[a]Total trailing-edge section angle of 8°.

TABLE III

WEIGHT, BALANCE, AND INERTIA DATA FOR THE 1/5-SCALE ROCKET-PROPELLED MODELS OF THE CONVAIR YF-102 AND F-102A AIRPLANES

	YF-102	F-102A
Weight (propellant expended), lb	352	403
Wing loading, lb/sq ft	13.3	15.2
Center of gravity:		
Longitudinal, percent $\bar{c}$	21.9	22.0
Lateral, from plane of symmetry, in.	-0.1	0.06
Vertical, from reference line, in.	-1.4	-0.6
Moment of inertia:		
About X principal axis, slug-ft^2	8	----
About Y principal axis, slug-ft^2	75	108
About Z principal axis, slug-ft^2	51	----
Principal-axis inclination (down at nose from wing chord plane), deg	$\approx$ 1.2	----

TABLE IV

EXTERNAL-PRESSURE-DRAG COEFFICIENTS $C_{D_{p+b}}$ AT M = 1.05 AND 1.2 FROM FREE-FLIGHT TESTS OF SEVERAL VARIATIONS OF THE CONVAIR F-102 CONFIGURATION

Airplane	Equivalent-body model	External-pressure-drag coefficient,[a] $C_{D_{p+b}}$, for M = 1.05	
		Equivalent body of revolution	1/5-scale rocket-propelled model
Basic	1	0.0179	------
YF-102	2	.0183	0.0190
2-foot fuselage extension	3	.0181	------
F-102A	4	.0137	.0149
YF-102 (M = 1.2)	5	[b].0159	[b].0196
F-102A (M = 1.2)	6	[b].0115	[b].0163
F-102A, relocated inlets	7	.0113	------
F-102A, faired nose	8	.0116	------
F-102A, parabolic nose	9	.0108	------

[a]This parameter is a measure of drag rise and includes base drag.

[b]Values for M = 1.2.

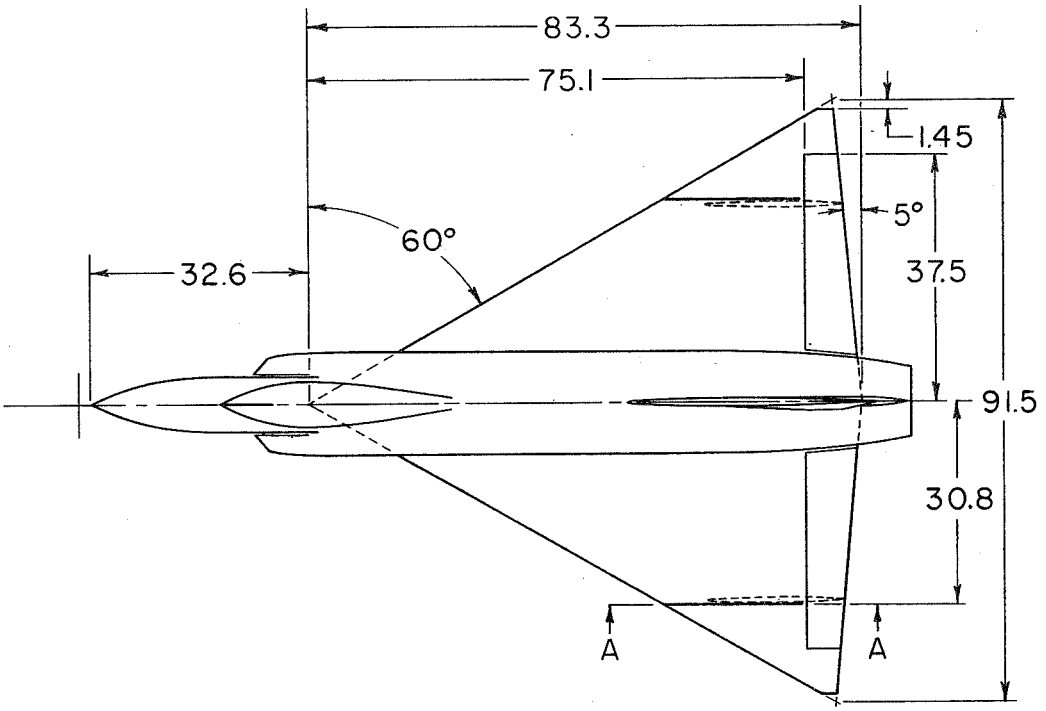

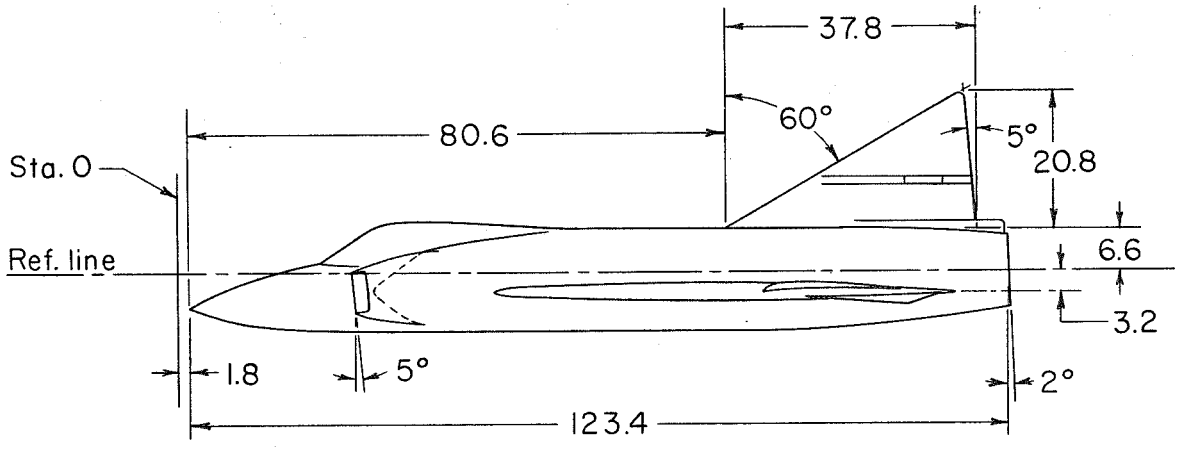

(a) Dimensional details of the 1/5-scale model of the Convair YF-102 airplane.

Figure 1.- General arrangement of the 1/5-scale rocket-propelled models of the Convair F-102 configuration. All dimensions are in inches.

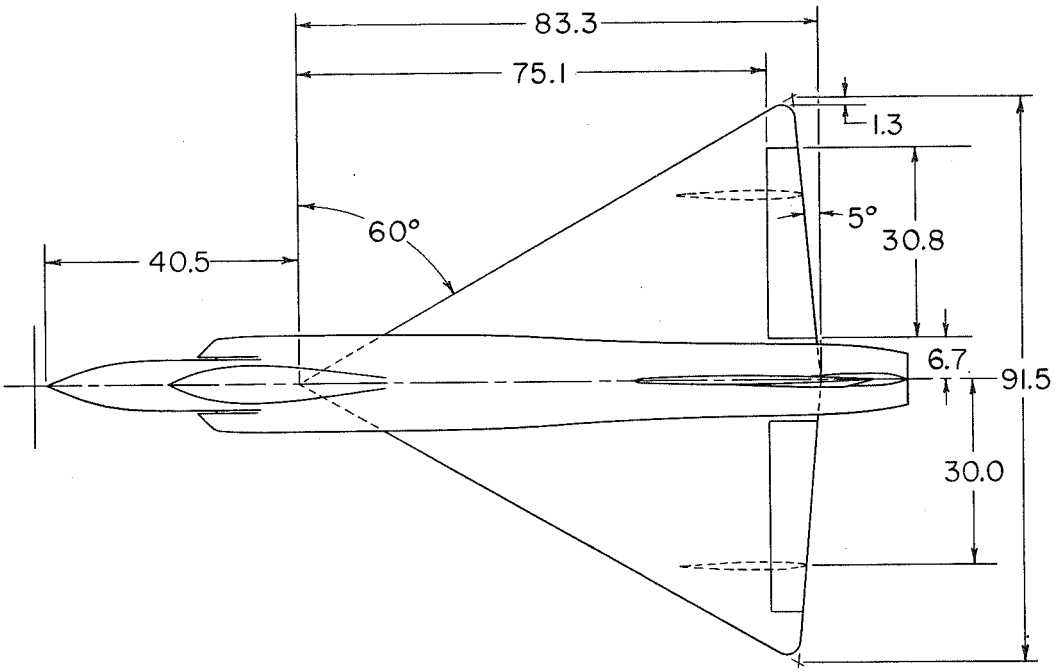

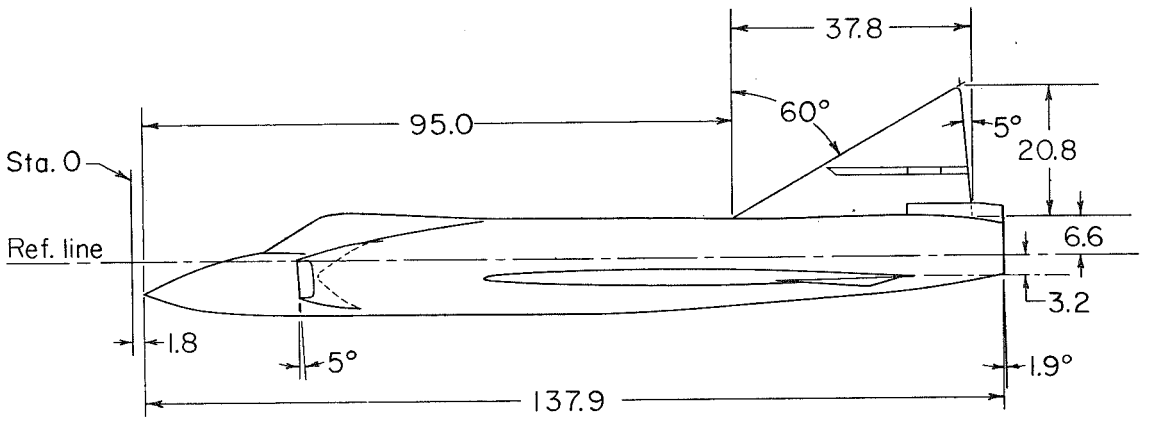

(b) Dimensional details of the 1/5-scale model of the Convair F-102A airplane.

Figure 1.- Concluded.

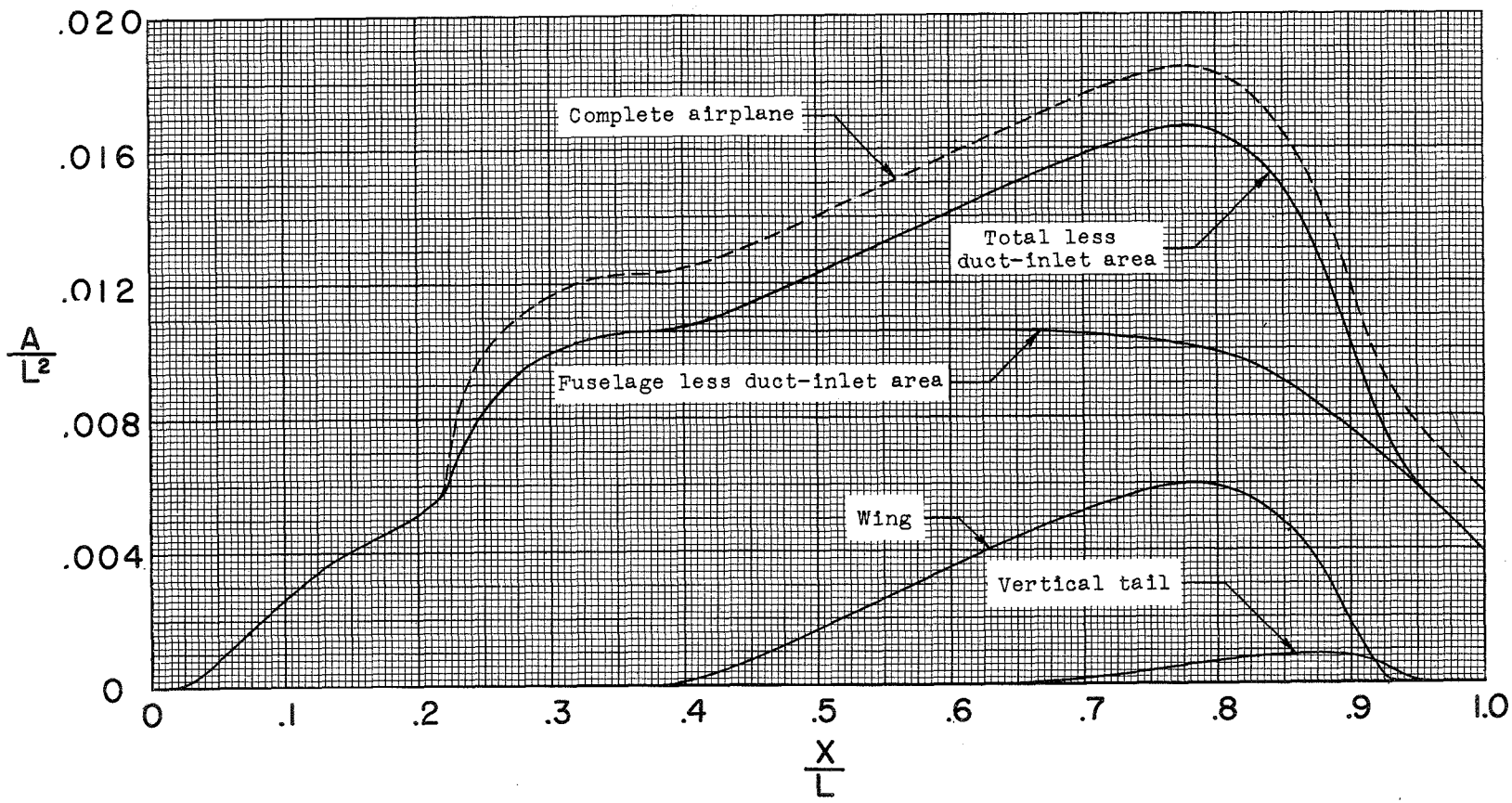

(a) YF-102 model. L = 125.2 inches.

Figure 2.- Longitudinal distribution of cross-sectional area of the 1/5-scale models.

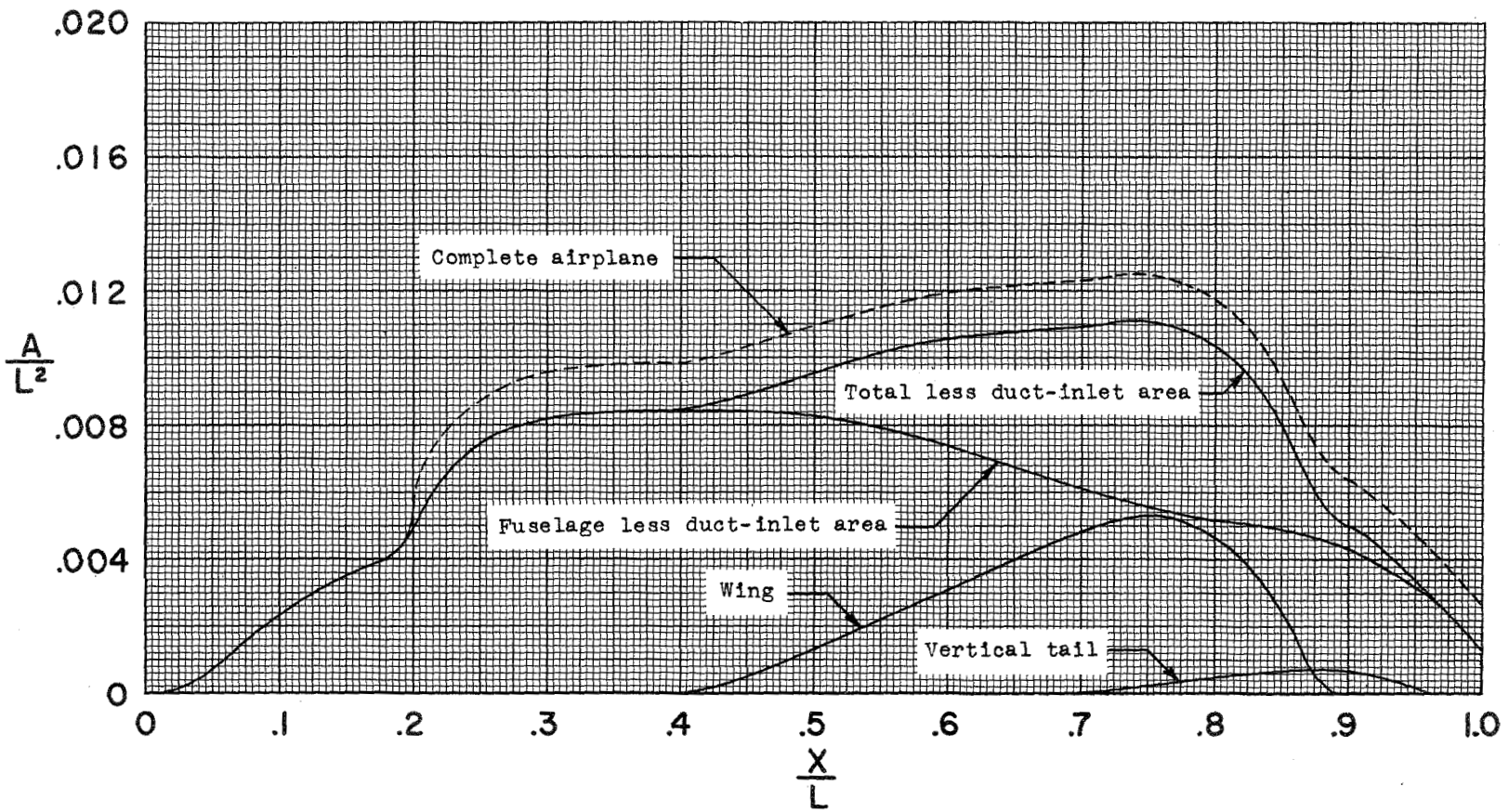

(b) F-102A model. L = 139.7 inches.

Figure 2.- Concluded.

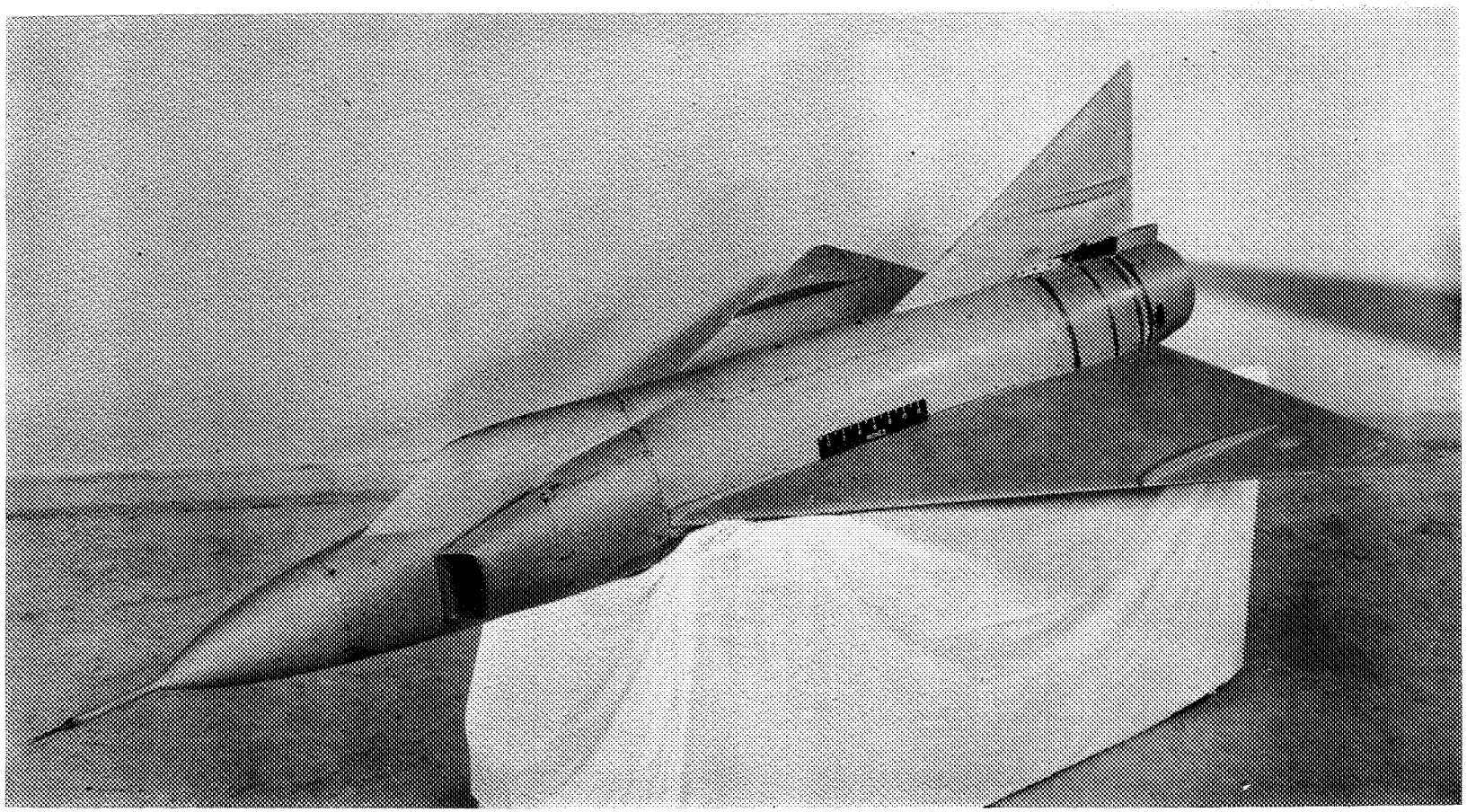

L-81068

(a) Overall view of the model of the YF-102.

Figure 3.- Photographs of the 1/5-scale models.

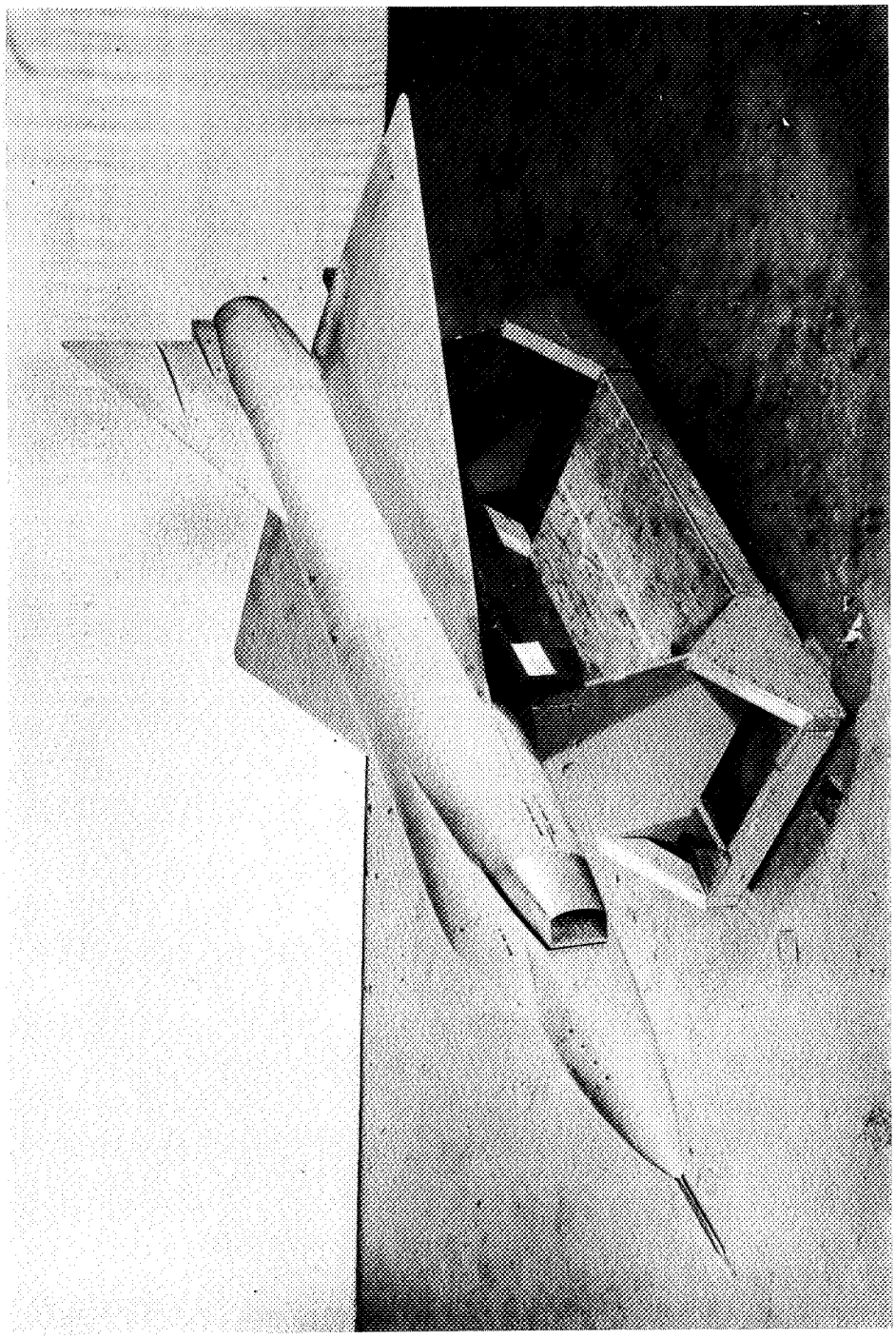

L-83108

(b) Overall view of the model of the F-102A.

Figure 3.- Continued.

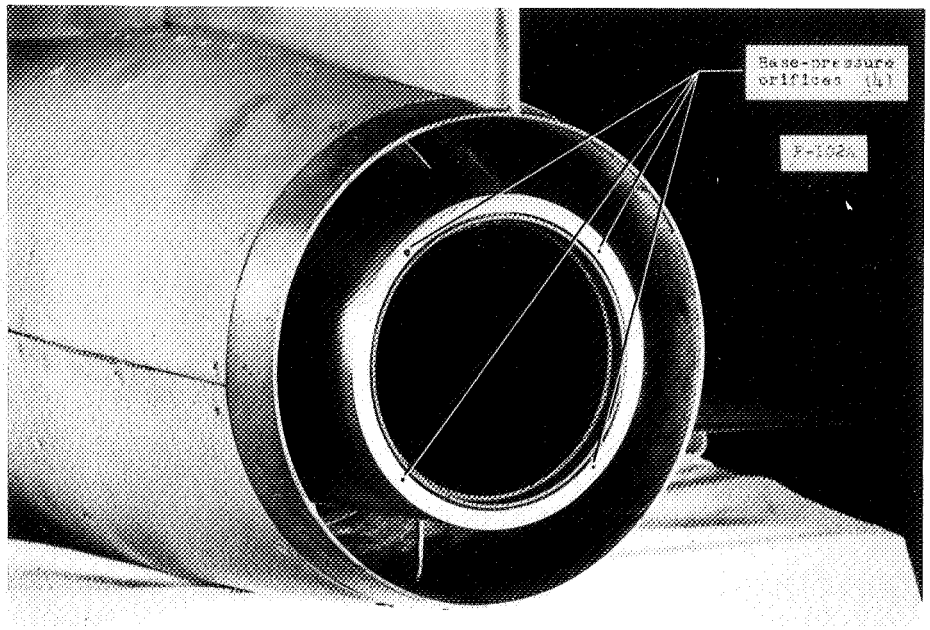

L-83109.1

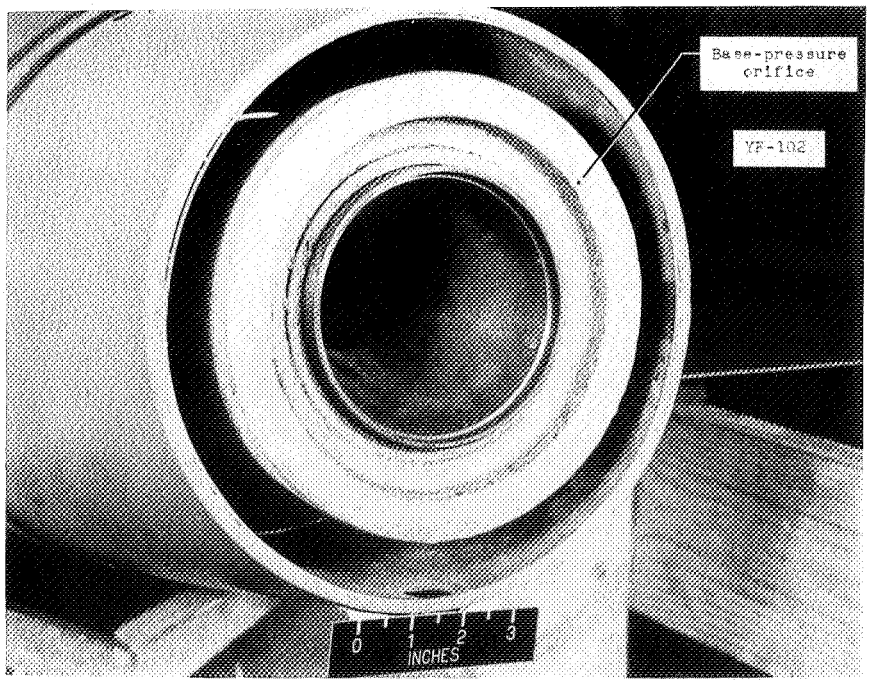

L-81067.1

(c) Views showing the duct exit of each 1/5-scale model.

Figure 3.- Continued.

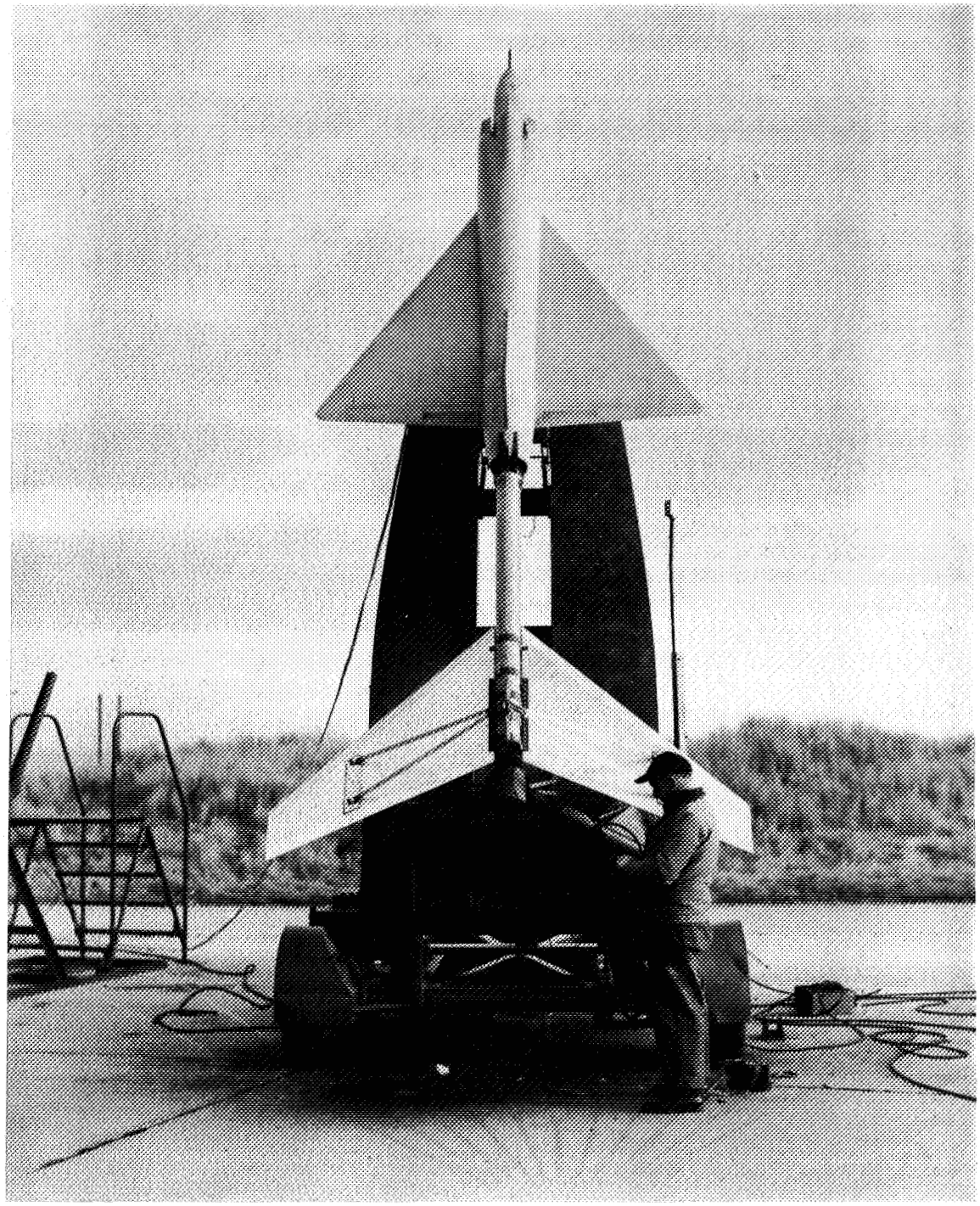

L-83429

(d) The 1/5-scale model of the Convair F-102A airplane on the launcher.

Figure 3.- Concluded.

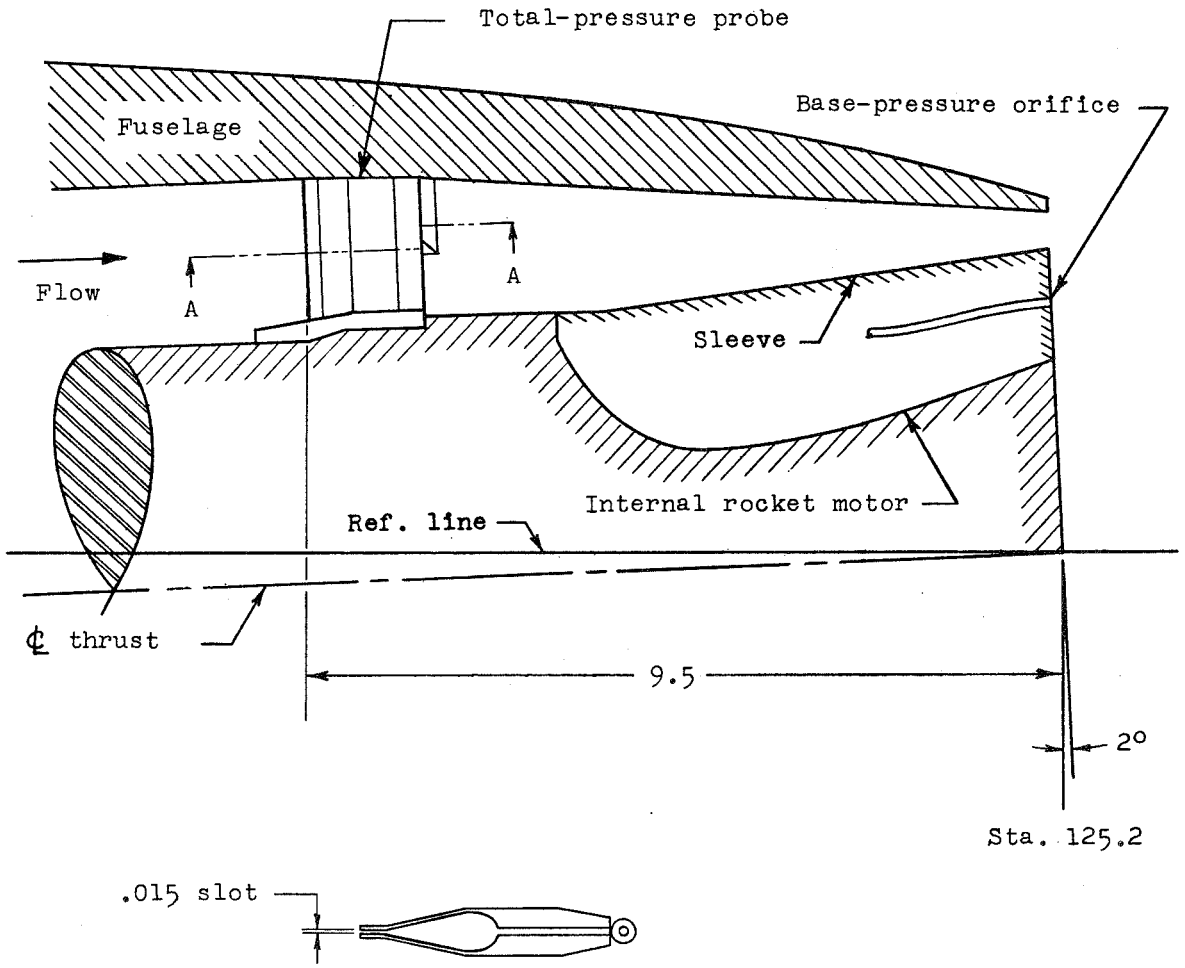

Section A-A

Figure 4.- Installation of duct-exit total-pressure probe. YF-102 model shown; F-102A model similar.

Model	L
1	9.956
2	10.283
3	10.350
4	11.246
5	10.283
6	11.246
7	11.246
8	11.246
9	11.246

Scale = 0.01643 (linear)

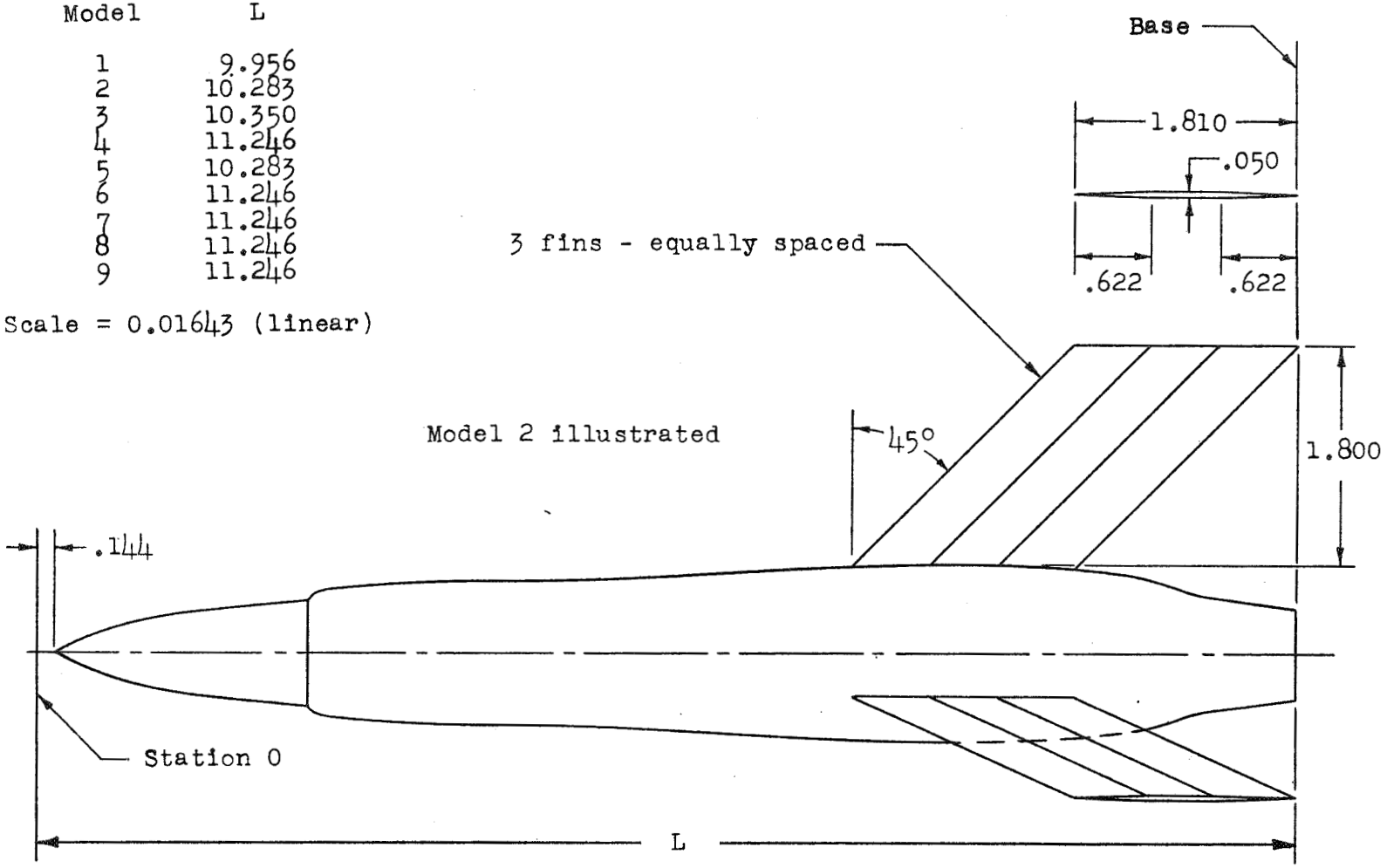

Figure 5.- Size, shape, and location of the equivalent-body-model stabilizing fins. Same for models 1 to 9. All dimensions are in inches.

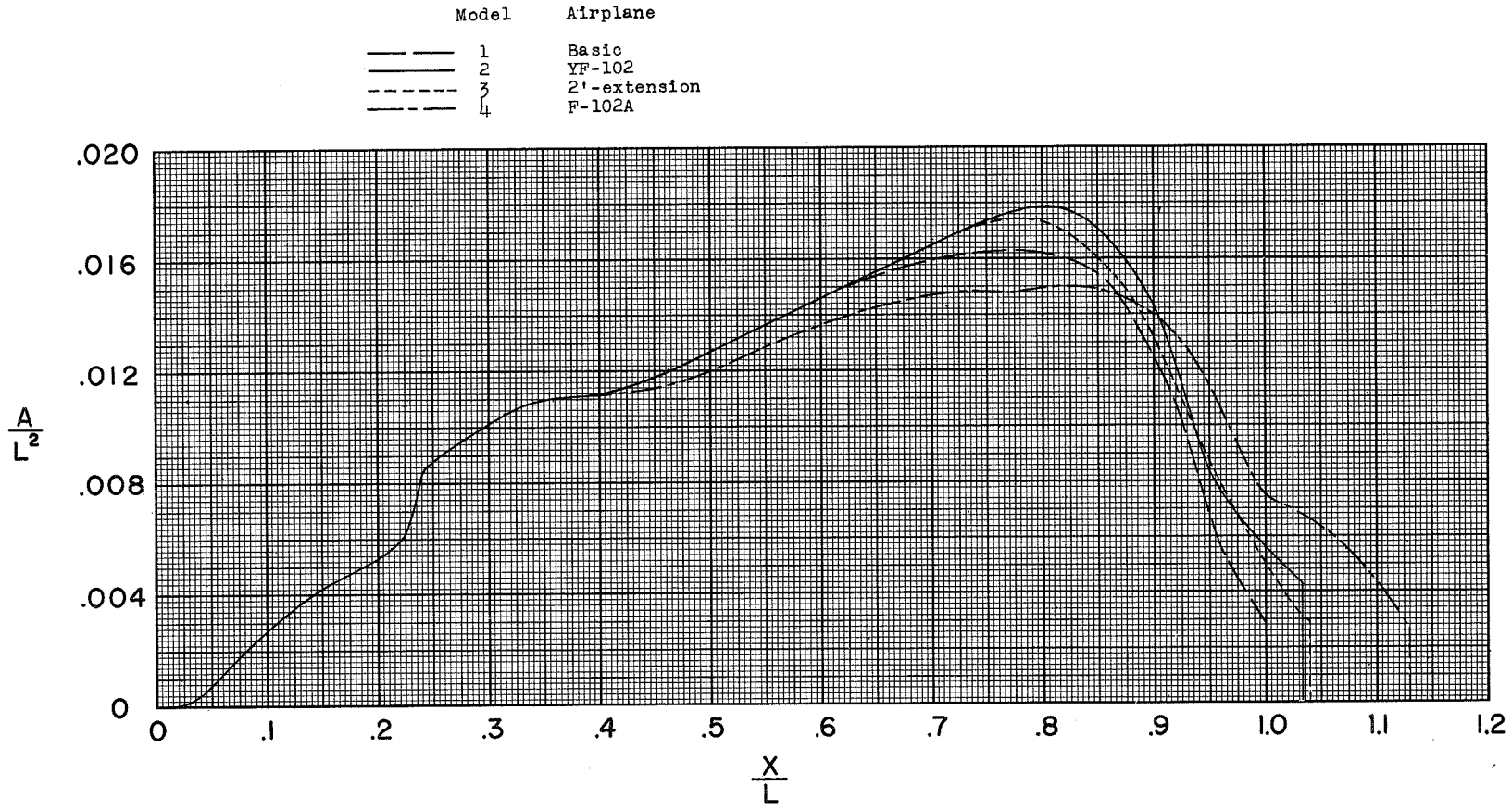

(a) Models 1 to 4 (M = 1.0). L = 9.956 (basic).

Figure 6.- Longitudinal distribution of cross-sectional area for the equivalent-body models.

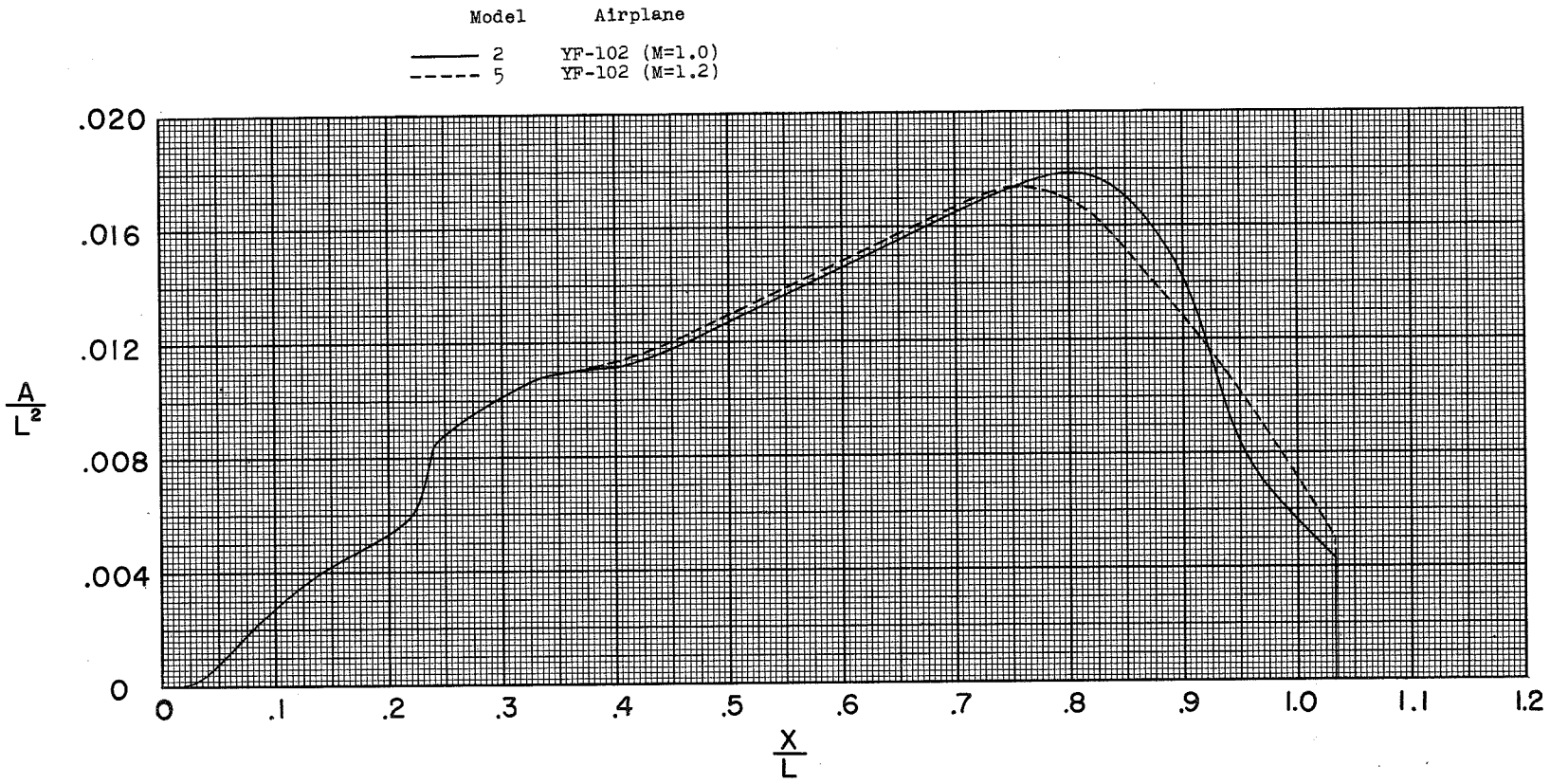

(b) Models 2 (M = 1.0) and 5 (M = 1.2). L = 9.956 (basic).

Figure 6.- Continued.

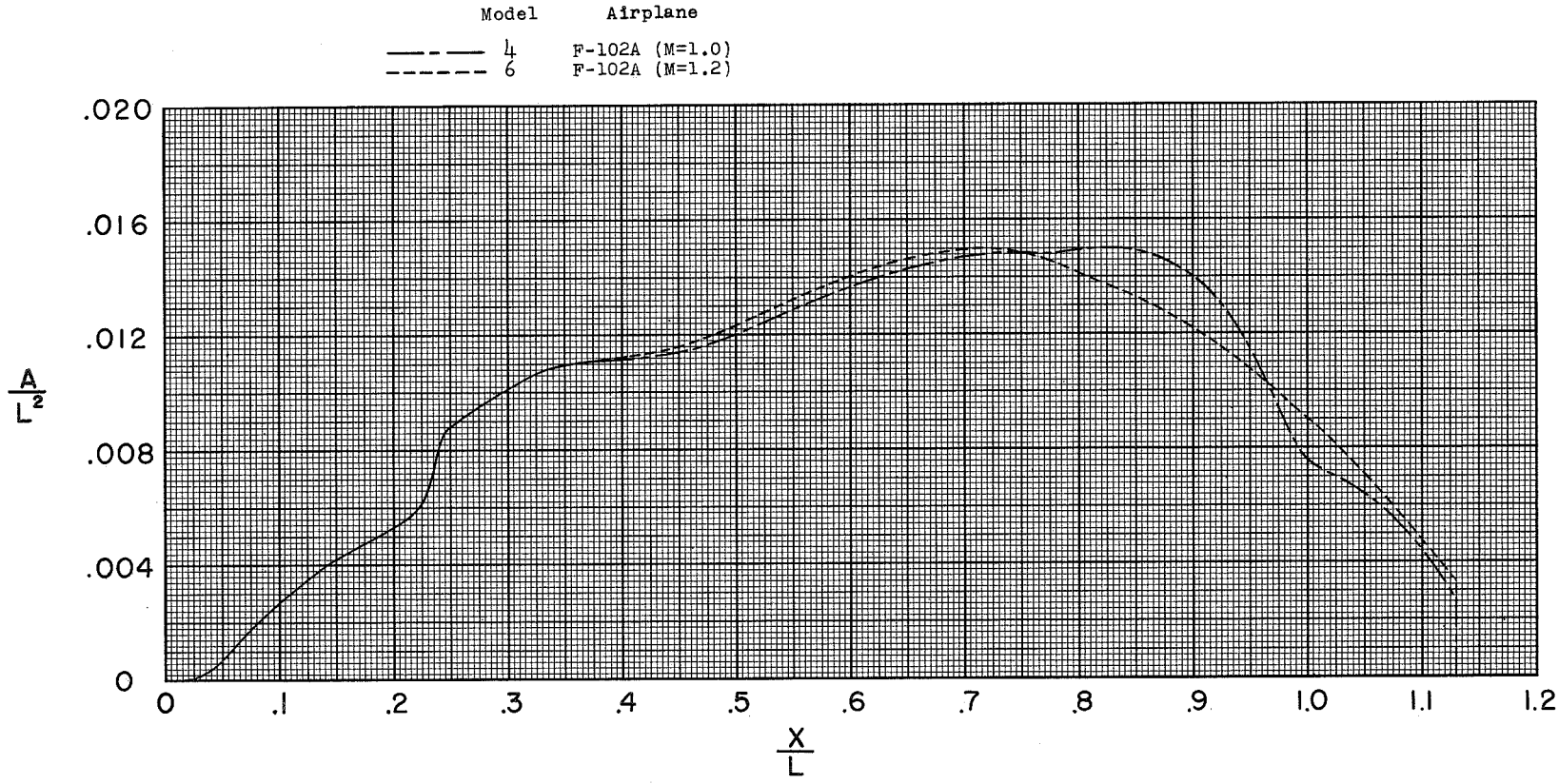

(c) Models 4 (M = 1.0) and 6 (M = 1.2). L = 9.956 (basic).

Figure 6.- Continued.

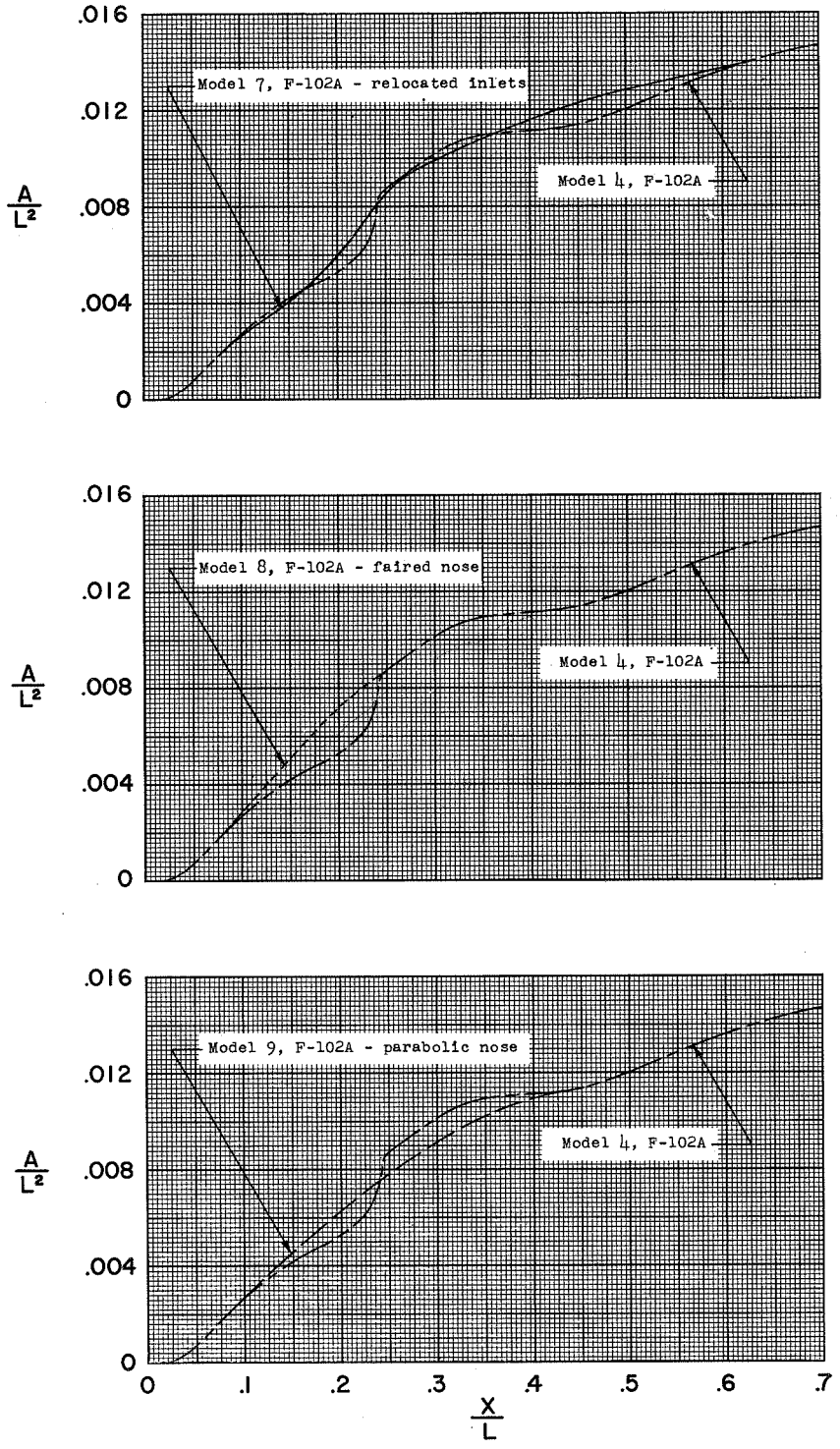

(d) Models 4 and 7 to 9 (M = 1.0). L = 9.956 (basic).

Figure 6.- Concluded.

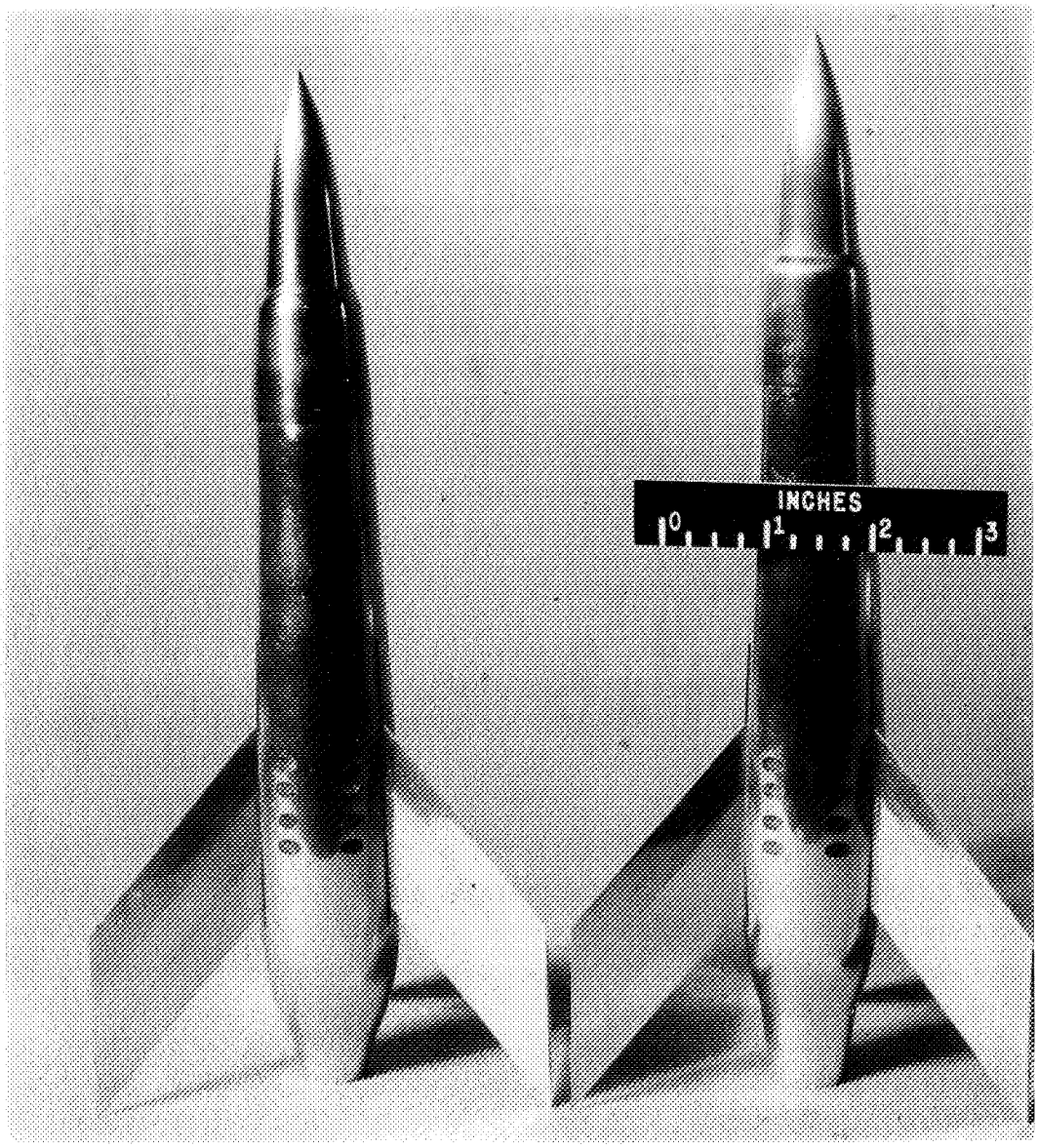

L-80864

(a) Models 1 and 2.

Figure 7.- Photographs of typical equivalent-body models.

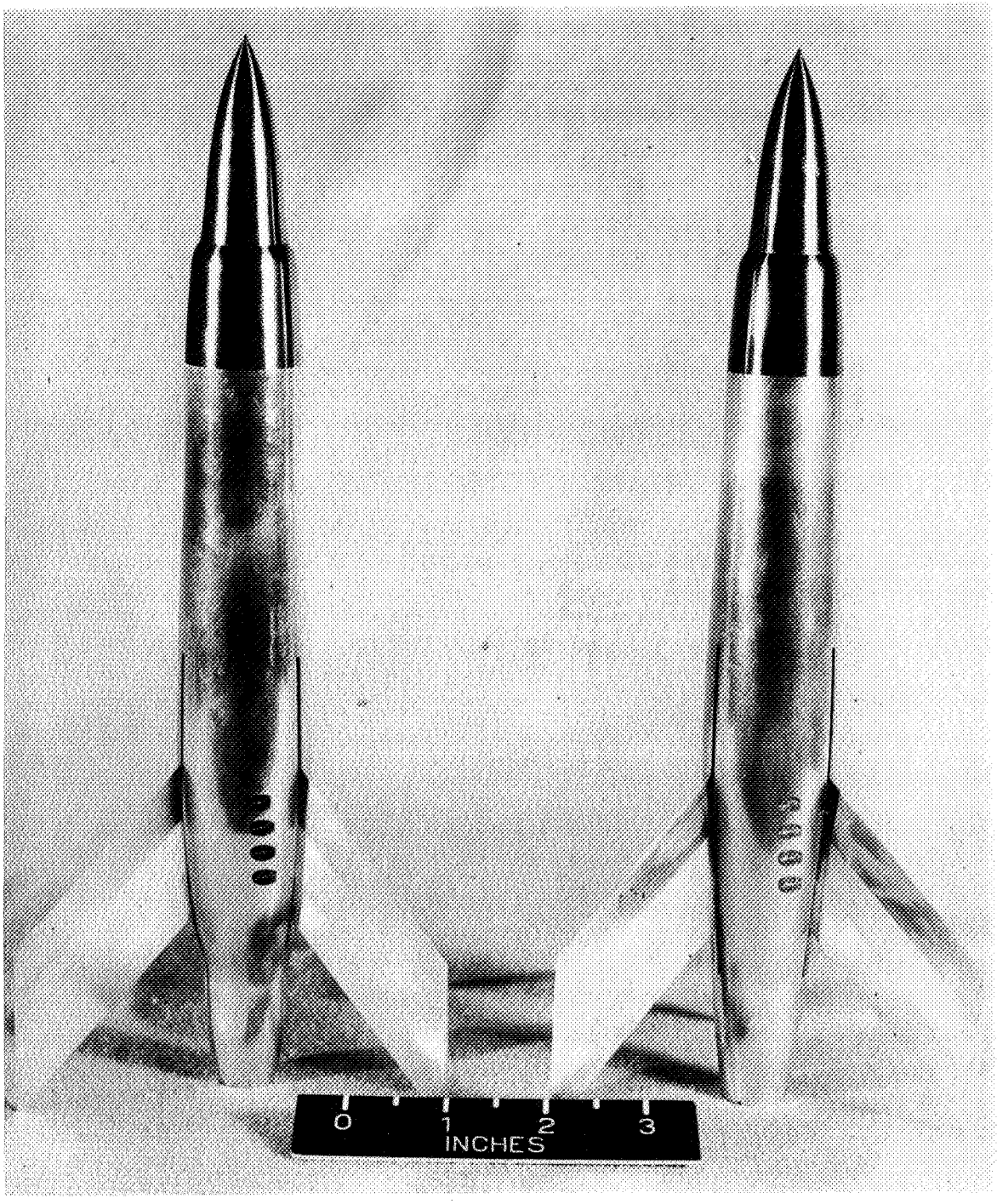

L-81776

(b) Models 4 and 6.

Figure 7.- Concluded.

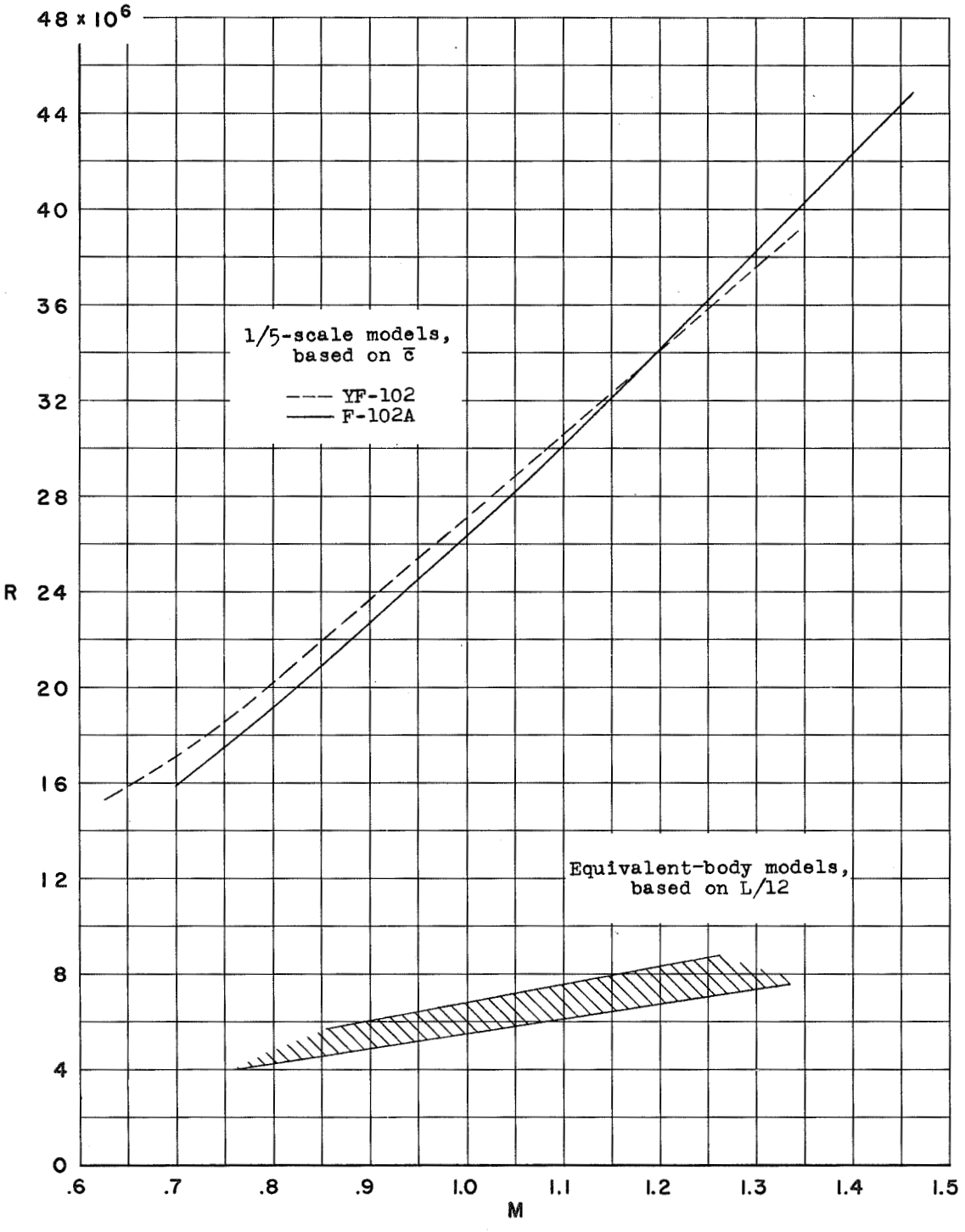

Figure 8.- Variation of Reynolds number with Mach number for the 1/5-scale and equivalent-body models.

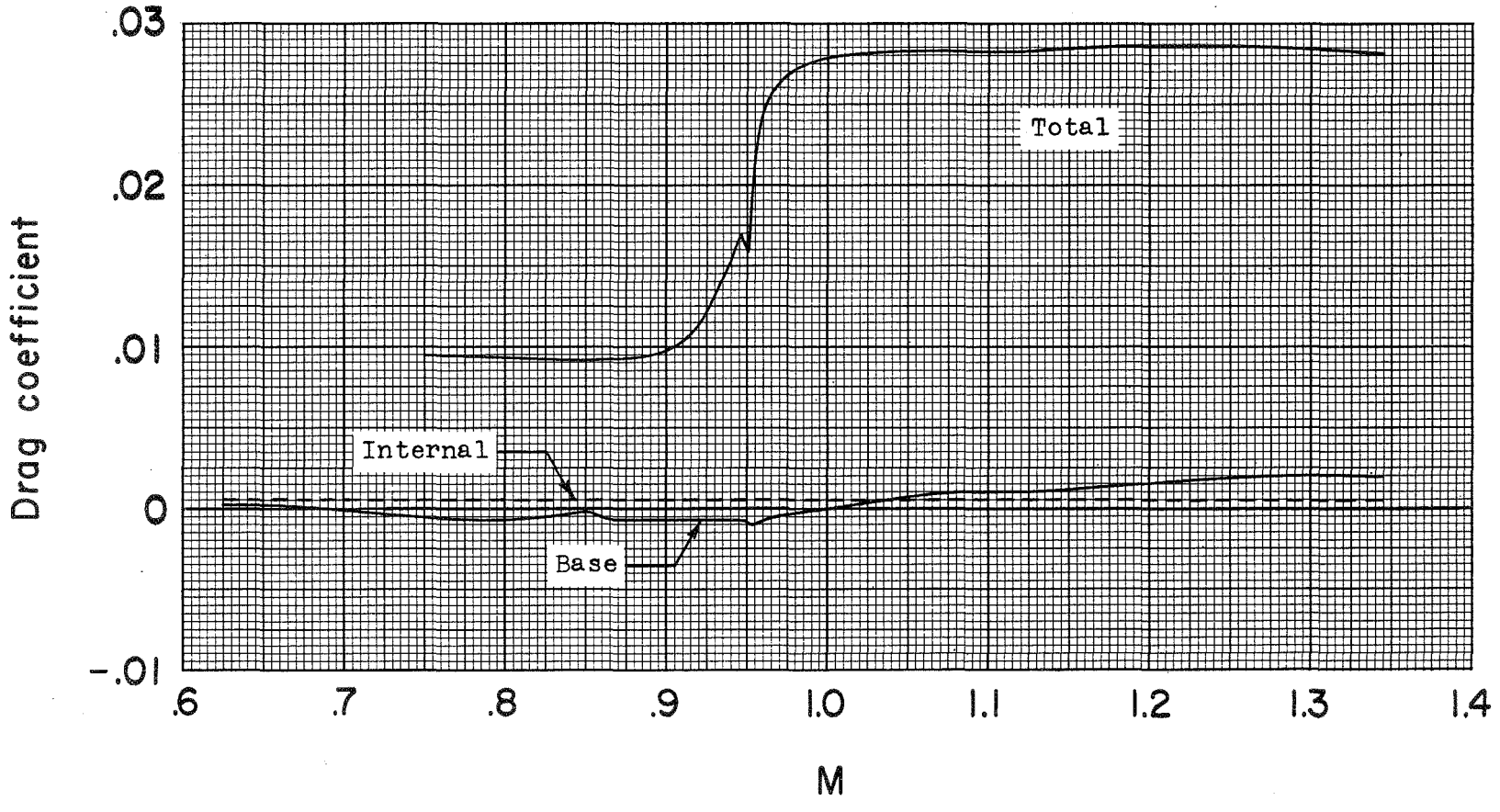

(a) Total-drag (C_D), internal-drag (C_{D_I}), and base-drag (C_{D_b}) coefficients.

Figure 9.- Variation with Mach number of the measured drag characteristics of the 1/5-scale model of the Convair YF-102 airplane.

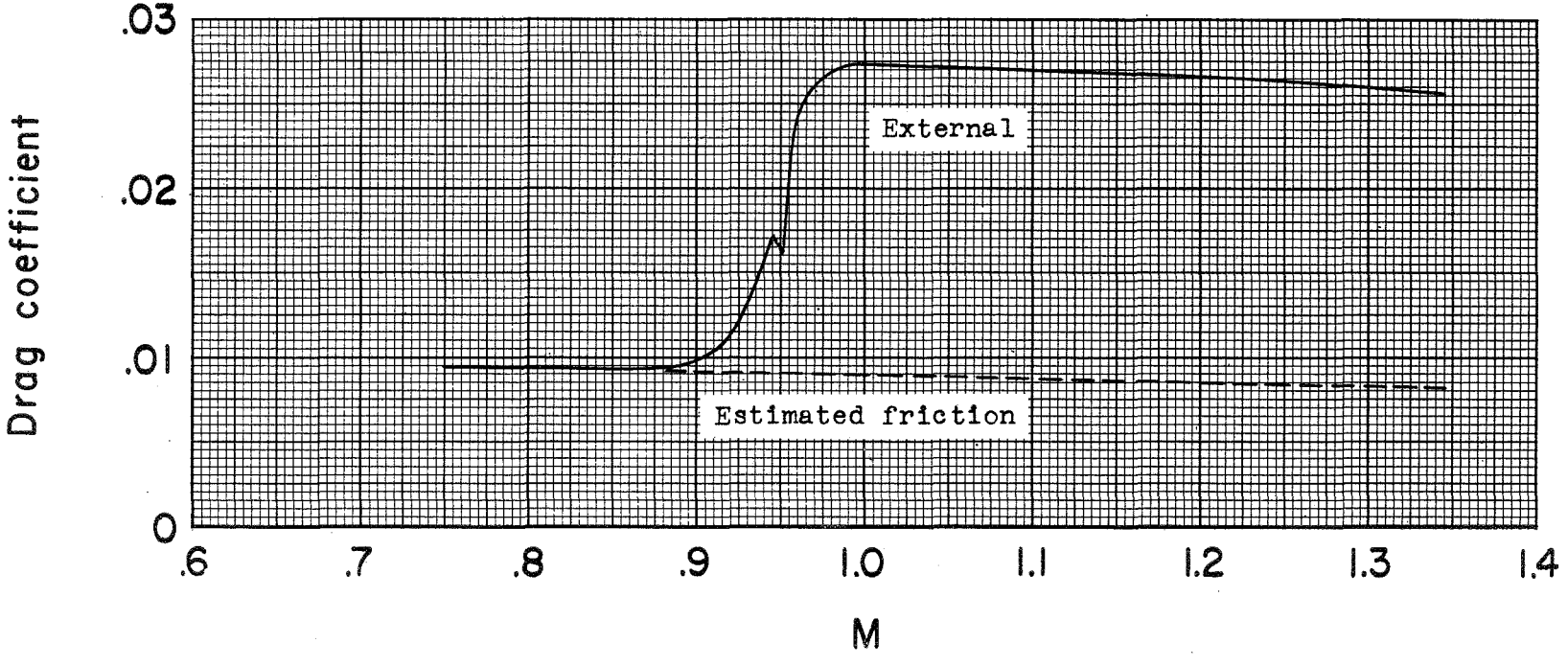

(b) Forebody external-drag coefficients C_{D_E} and estimated external friction-drag coefficients C_{D_f}.

Figure 9.- Concluded.

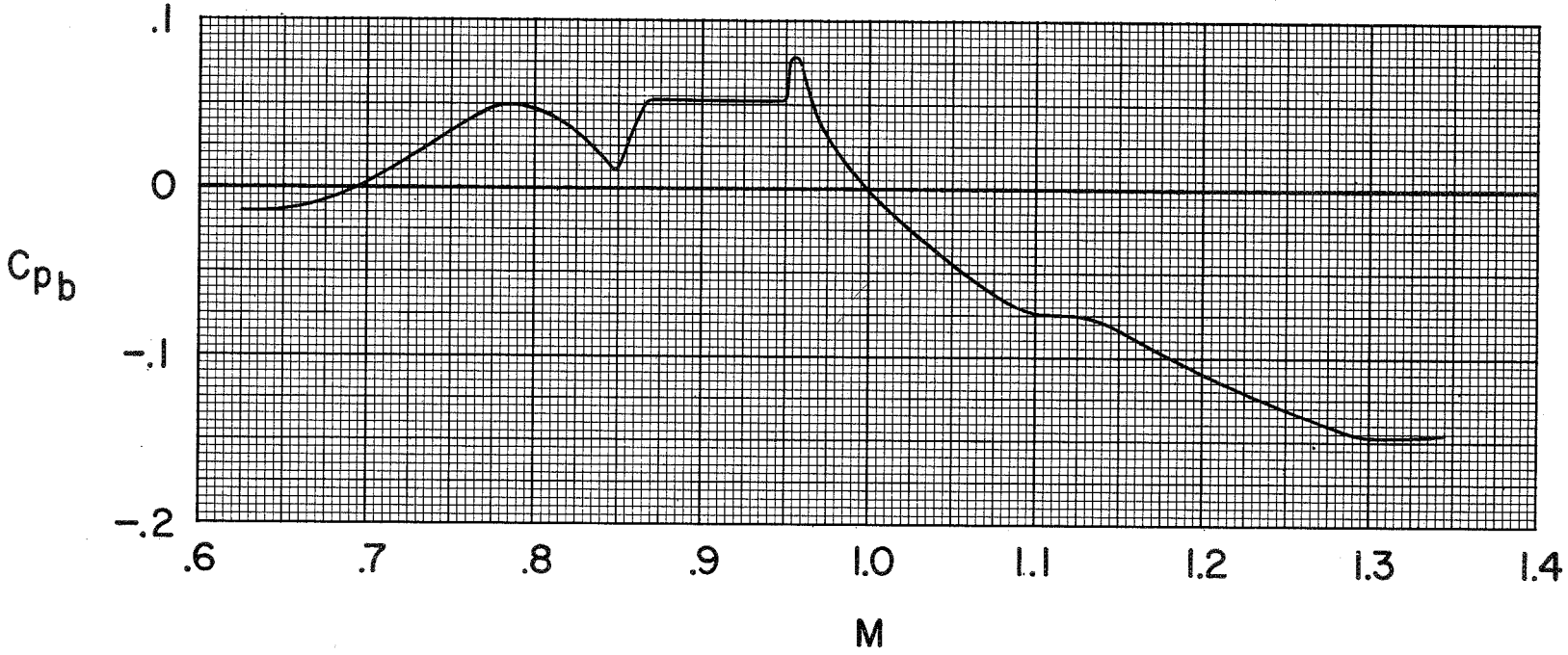

Figure 10.- Measured base pressure coefficients from the 1/5-scale model of the YF-102 airplane.

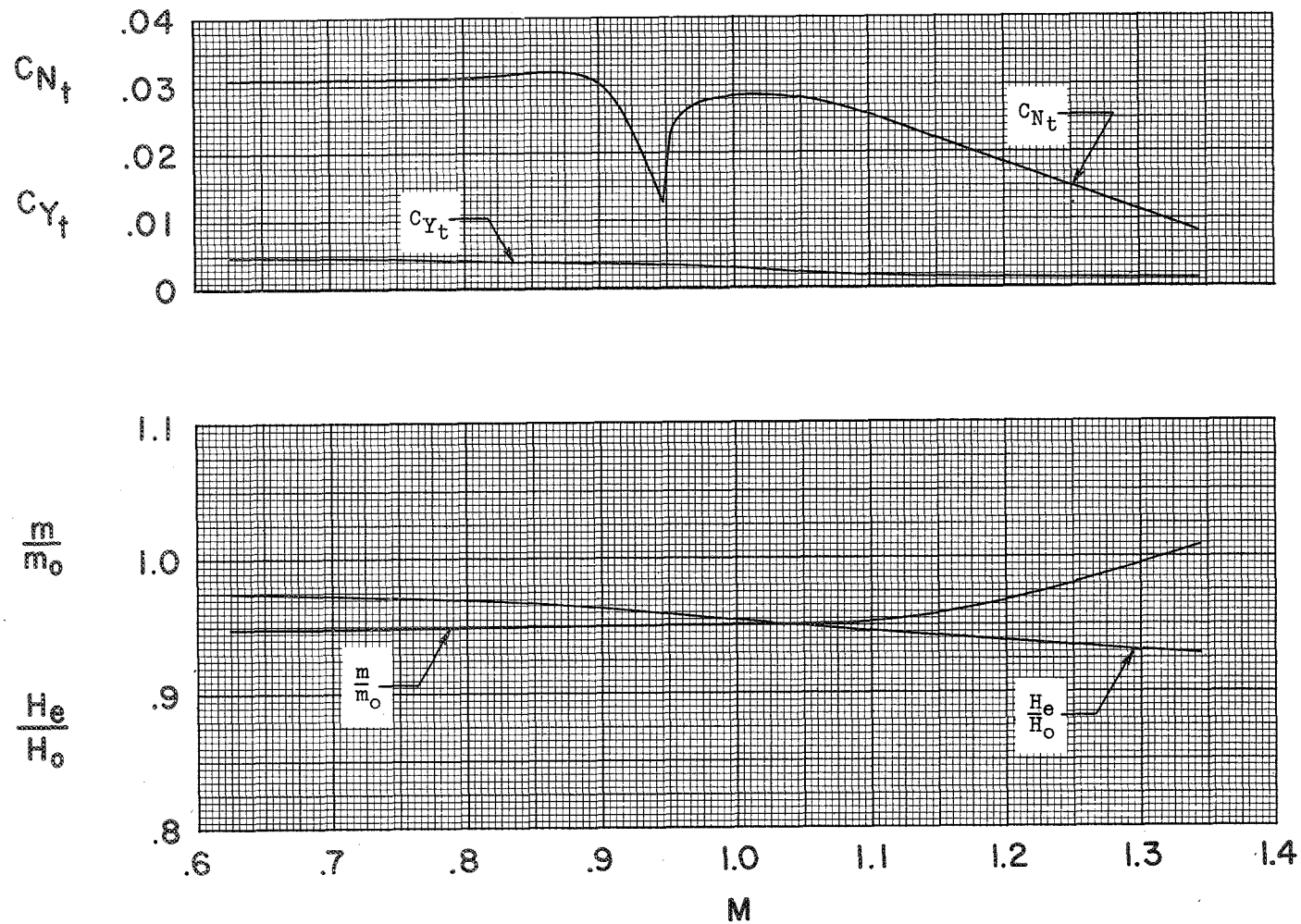

Figure 11.- Trim normal- and side-force coefficients and duct pressure-recovery and mass-flow ratios plotted against Mach number for the 1/5-scale model of the Convair YF-102 airplane.

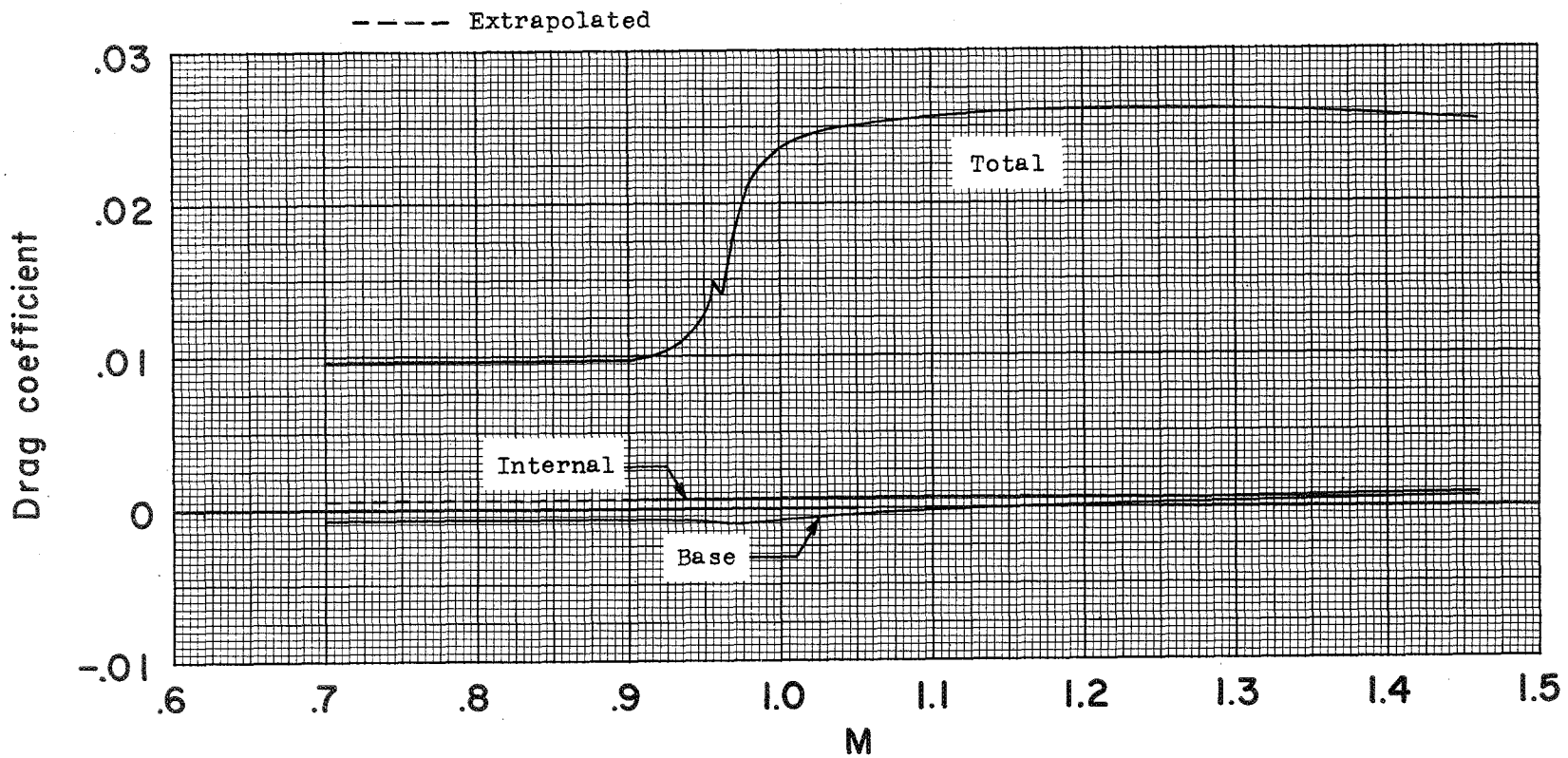

(a) Total-drag (C_D), internal-drag (C_{D_I}), and base-drag (C_{D_b}) coefficients.

Figure 12.- Variation with Mach number of the measured drag characteristics of the 1/5-scale model of the Convair F-102A airplane.

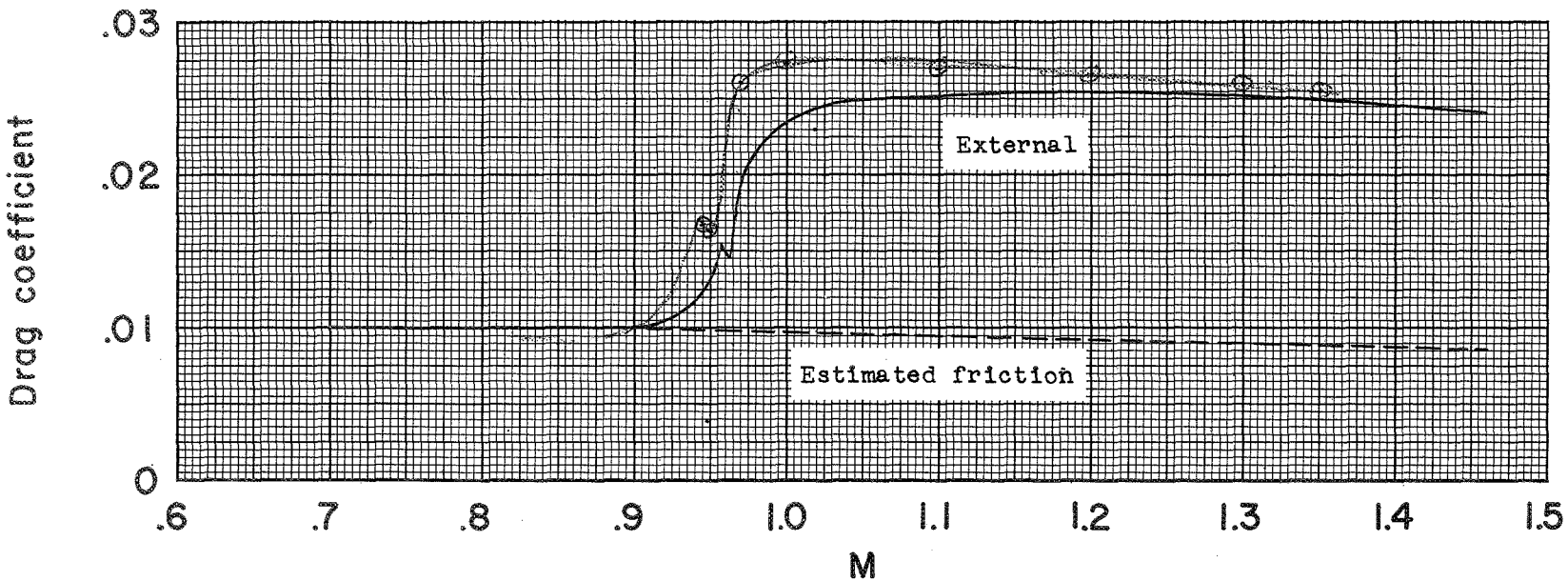

(b) Forebody external-drag coefficients C_{D_E} and estimated external friction-drag coefficients C_{D_f}.

Figure 12.- Concluded.

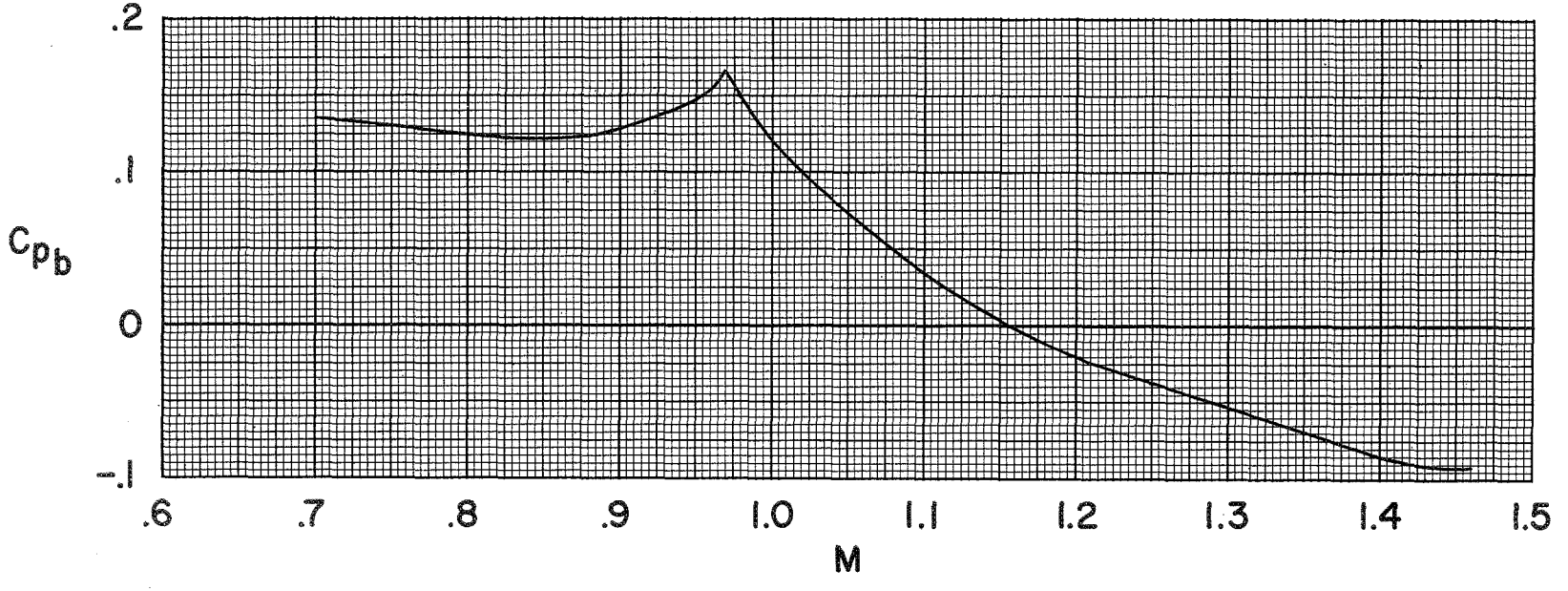

Figure 13.- Measured base pressure coefficients from the 1/5-scale model of the F-102A airplane.

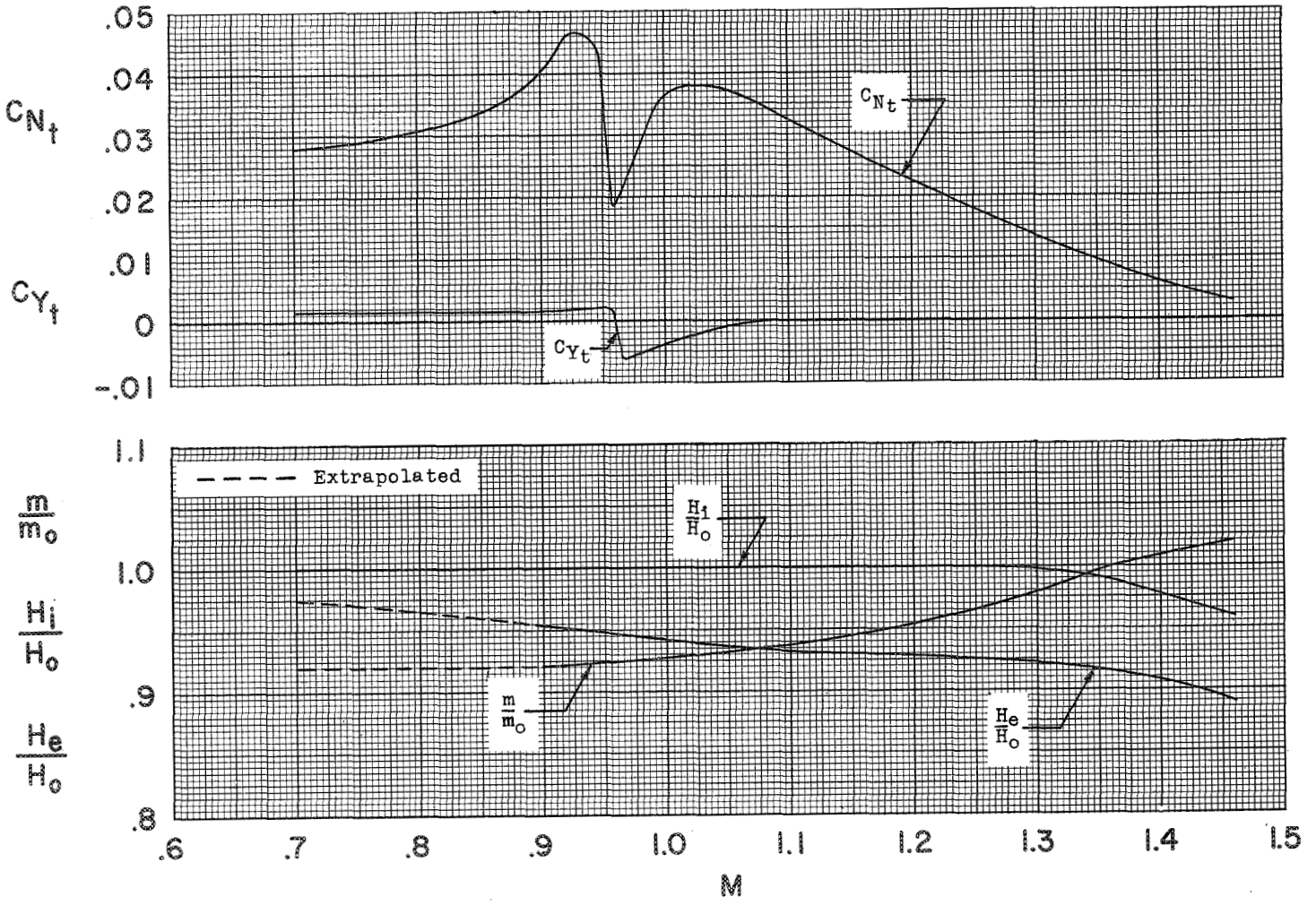

Figure 14.- Trim normal- and side-force coefficients and duct pressure-recovery and mass-flow ratios plotted against Mach number for the 1/5-scale model of the Convair F-102A airplane.

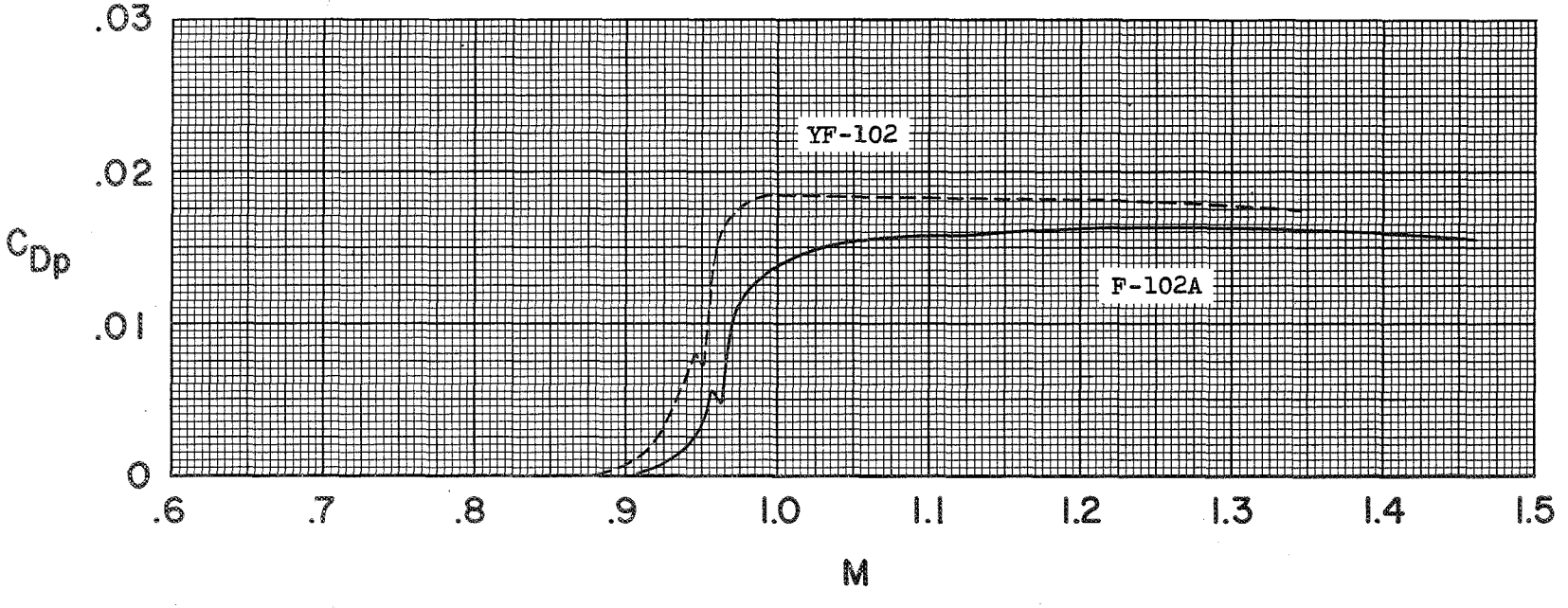

Figure 15.- Comparison of forebody external-pressure-drag coefficients from the 1/5-scale models of the Convair YF-102 and F-102A airplanes.

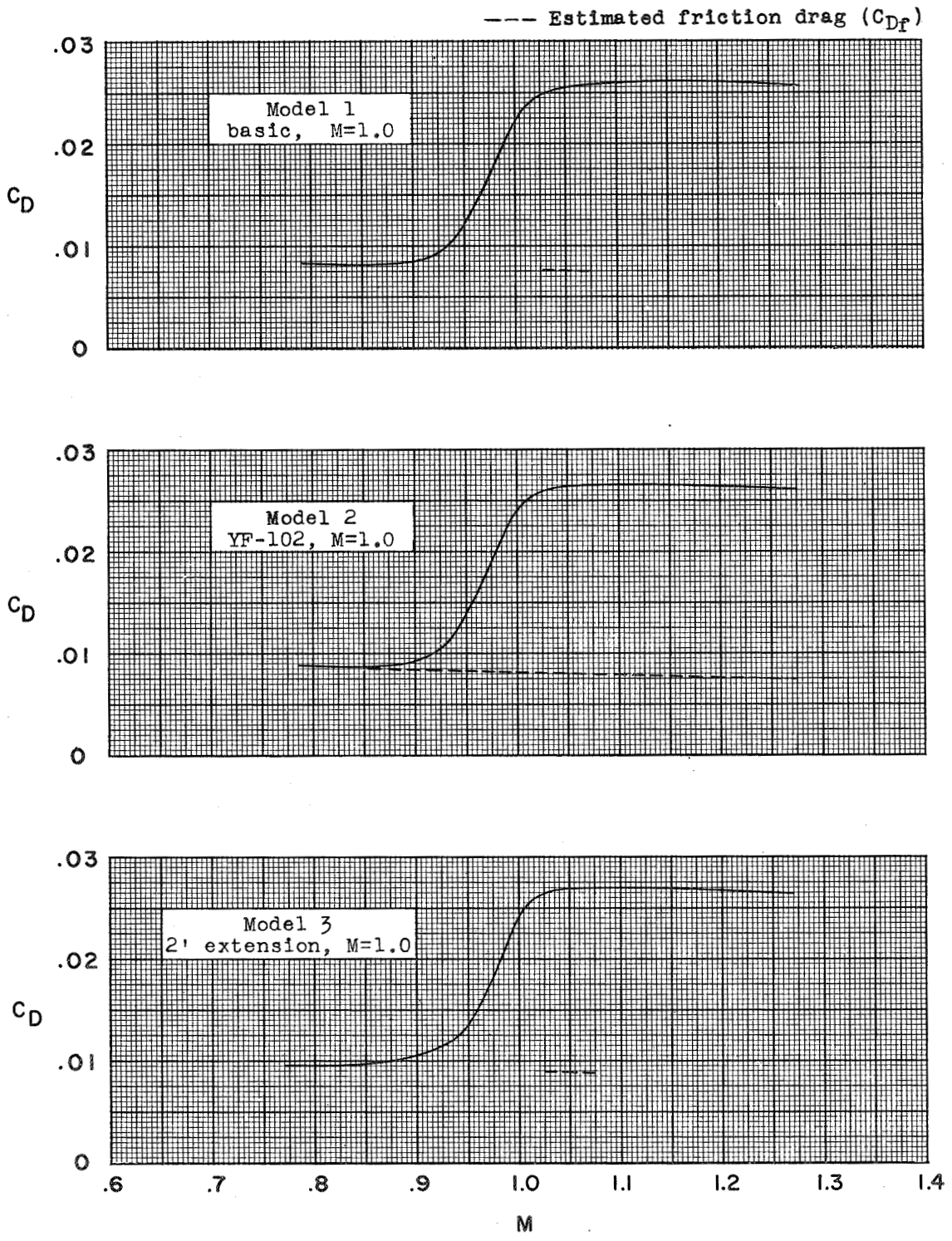

Figure 16.- Drag coefficients based on equivalent wing area from tests of nine equivalent-body-of-revolution models representing several variations of the Convair F-102 configuration.

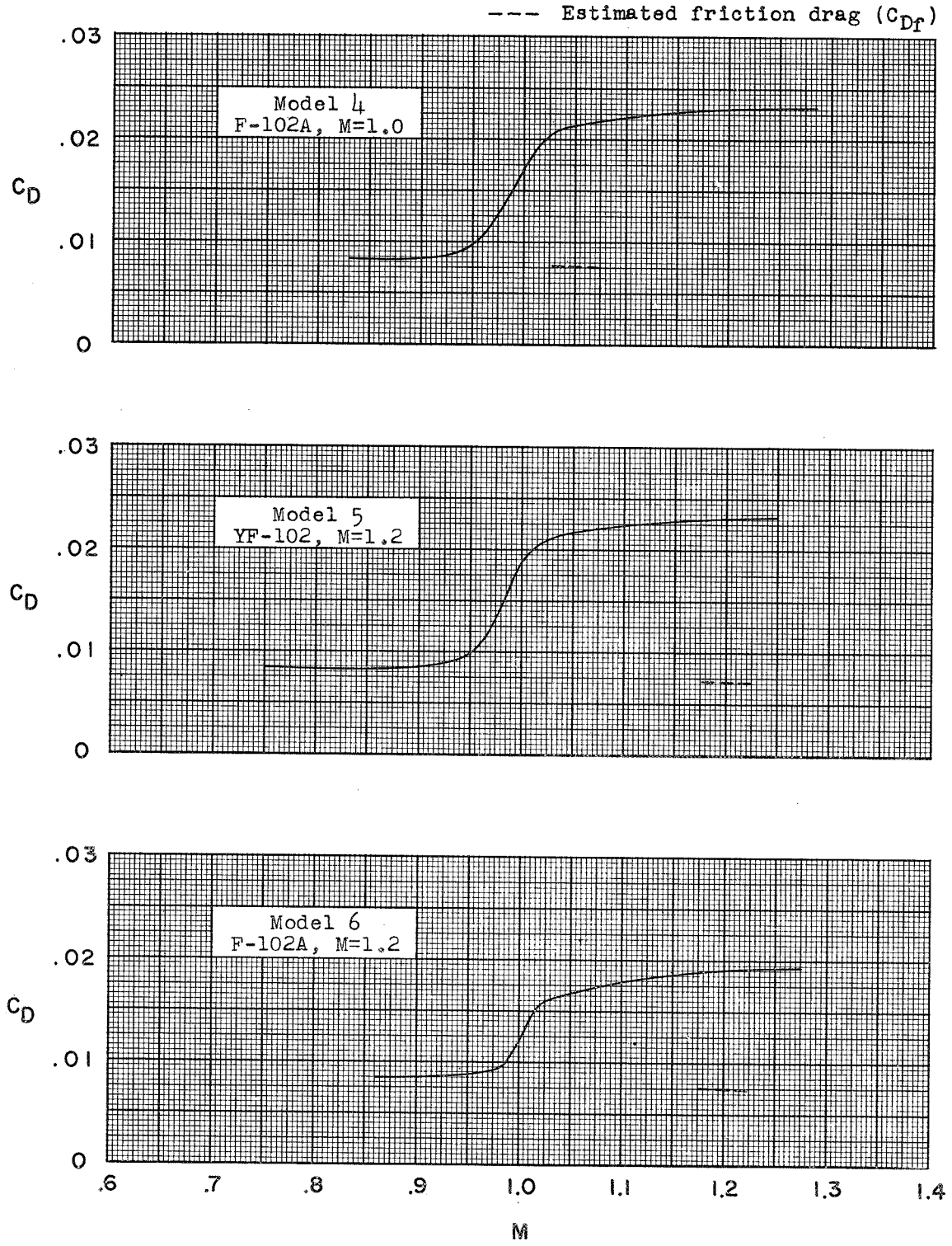

Figure 16.- Continued.

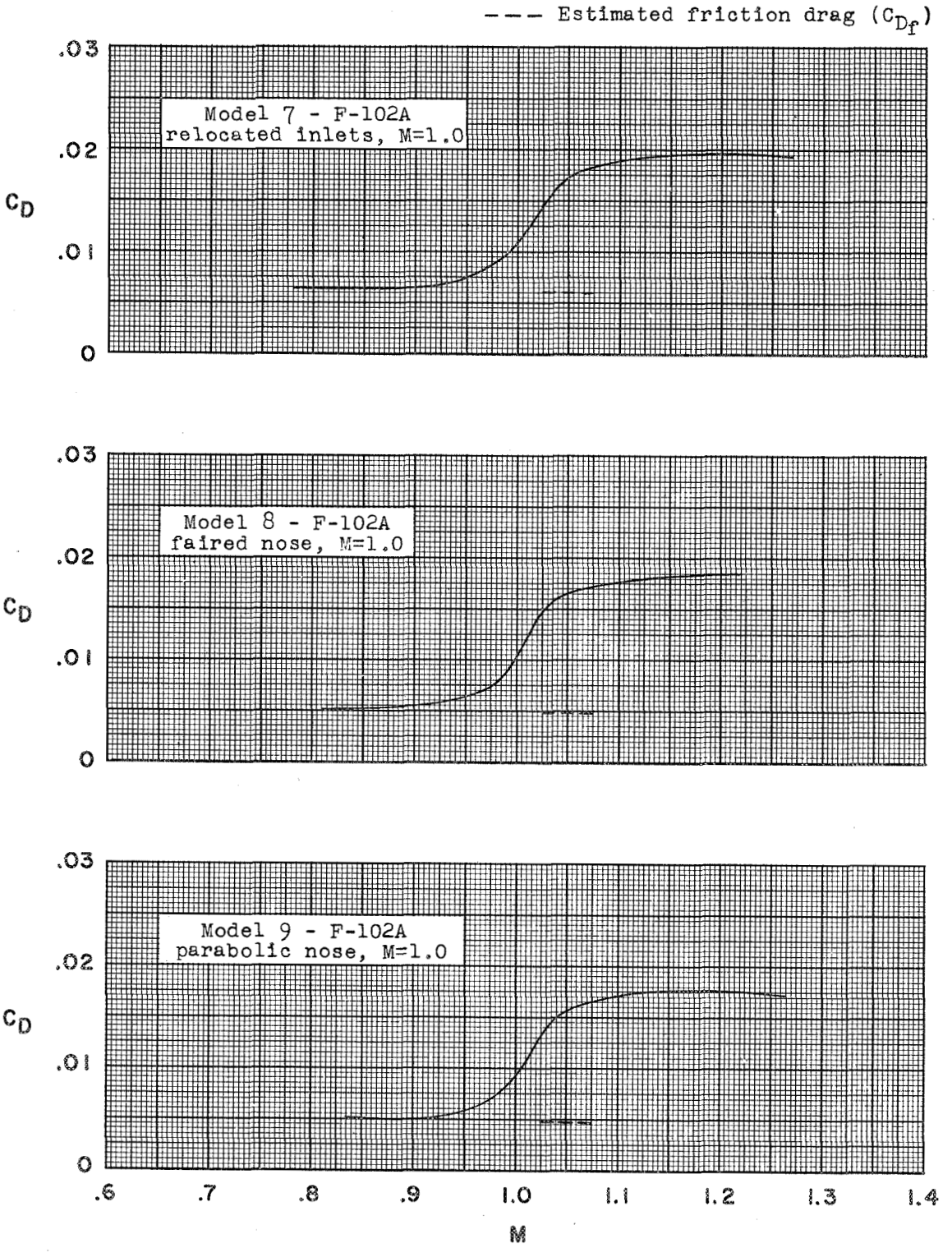

Figure 16.- Concluded.